THE INTERMETALLIC COMPOUNDS IN THE SILVER-STRONTIUM SYSTEM AND THEIR CRYSTAL STRUCTURES

Thesis by

Albert Charles Claus

In Partial Fulfillment of the Requirements
For the Degree of
Doctor of Philosophy

California Institute of Technology
Pasadena, California
1958

ACKNOWLEDGEMENTS

I am especially grateful to Professor B. G. Bergman for his cheerful assistance and for his patience.

I am also grateful to the Institute and the Office of Naval Research for their financial assistance.

Finally I would like to mention the enjoyable association with the other graduate students during my stay at the Institute.

ABSTRACT

Four congruently melting intermetallic compounds with the compositions Ag_4Sr, Ag_5Sr_3, AgSr and Ag_2Sr_3 respectively have been reported to exist in the silver-strontium system. In the present investigations the crystal structures of all four compounds were studied by application of X-ray diffraction techniques. The first compound was found to have the quite common $CaZn_5$ structure and the composition is Ag_5Sr rather than Ag_4Sr. The structure of the second compound has orthorhombic symmetry. It was not determined but there can hardly be any doubt that it is closely related to the C_{32} type (AlB_2 structure) and that the composition of the compound is Ag_2Sr and not Ag_5Sr_3. The third compound also has a structure of orthorhombic symmetry and is of a type not observed previously. The composition is correctly represented by the formula AgSr. The structure is partially disordered. The structure of the fourth compound was not determined in detail. It could, however, be established that it is very closely related to the AgSr structure. The composition Ag_2Sr_3 could be neither confirmed nor rejected. The structure has orthorhombic symmetry.

TABLE OF CONTENTS

I. INTRODUCTION

Weibke (1) investigated the phase diagram of the silver-strontium system by thermal analysis. His phase diagram shown in Figure 0 shows the existence of four different congruently melting intermetallic compounds of silver and strontium. According to Weibke they have the compositions Ag_4Sr, Ag_5Sr_3, AgSr and Ag_2Sr_3. No crystallographic investigation of these compounds seems to have been made.

The existence of as many as four congruently melting intermetallic compounds in a binary system is relatively rare. It may well be that the radius ratio of the silver and strontium atoms happens to be very near the ideal ratios for four structure types thus permitting the formation of no less than four compounds of relatively great stability. Other explanations can, of course, be advanced. It was in any case considered desirable that the atomic arrangements in the four compounds be determined, partly in an attempt to explain the presumed stability of the phases and partly to add information to the relatively incomplete body of knowledge about the structures of metals and alloys that existed at the time of the investigation.

All four of the intermetallic compounds were investigated, and the crystal structures of two of them (Ag_4Sr and AgSr) were completely determined. The two remaining structures proved to be of too great complexity to be completely determined in a reasonable length of time. The investigations were, however, carried far enough to establish the approximate atomic arrangements.

During the course of the work the Ag_4Sr compound was found to have the composition of Ag_5Sr and will hereafter be referred to as the Ag_5Sr compound.

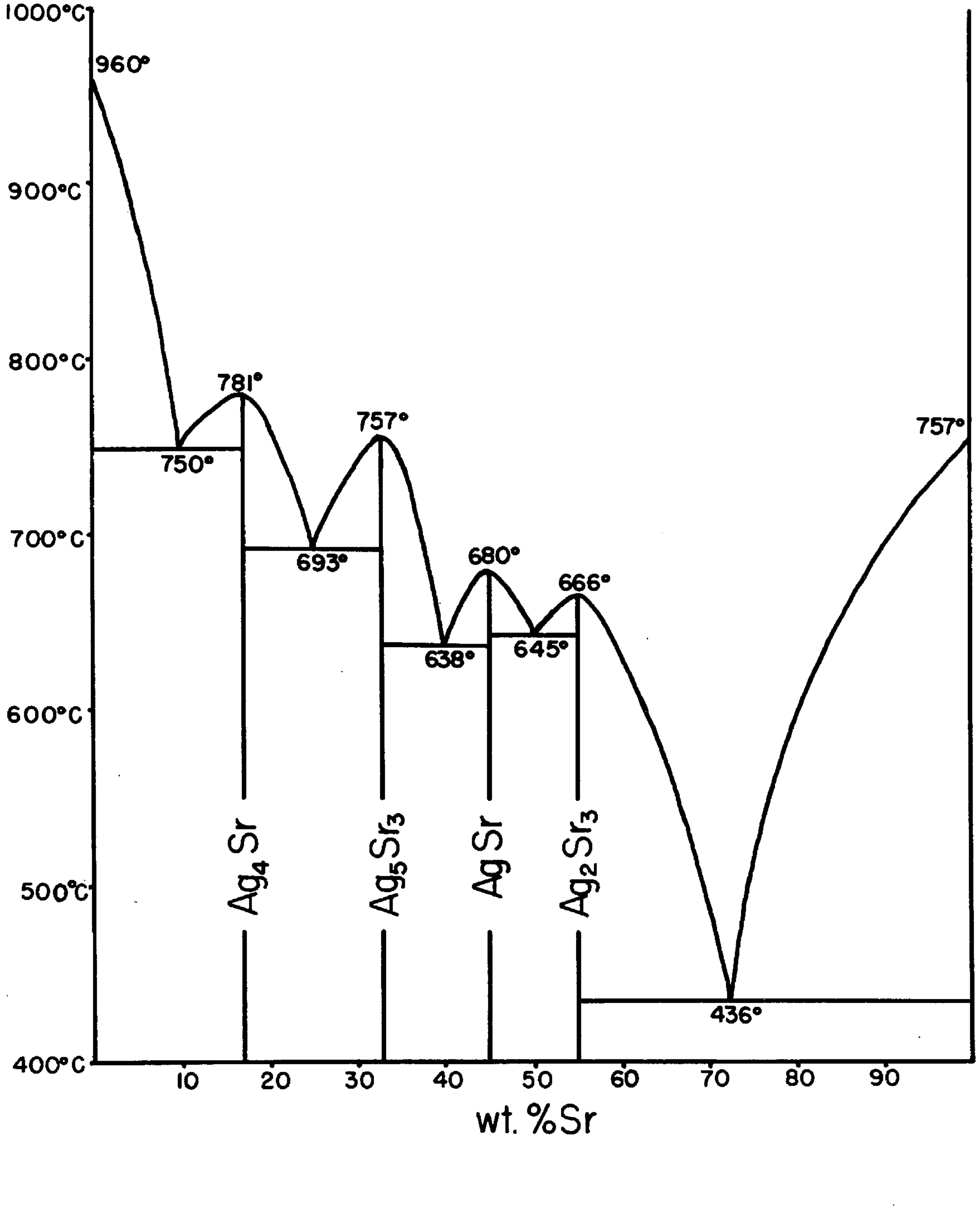

FIGURE 0. PHASE DIAGRAM OF SILVER-STRONTIUM

(Weibke, F., Z. Anorg. Allg. Chem., 193, p.301)

II. THE INTERMETALLIC COMPOUND Ag_5Sr

A. Materials

An alloy sample was prepared by melting 17.87 gm. of silver (99.99% pure) and 3.38 gm. of strontium (99.97% pure) in a sealed iron tube in an argon atmosphere.* An iron tube was chosen since neither silver nor strontium are soluble in iron to an appreciable extent (2), and an iron tube can be easily sealed.

The alloy was very brittle and had a silvery appearance. On exposure to air its color soon changed to a lustrous yellow. Otherwise the alloy appeared to be quite inert. From chemical analysis the composition of the alloy was found to correspond to $Ag_{5.03}Sr$. The silver content was determined by the Volhard method, and the strontium content was found by difference.

B. X-ray Photography and Laue Symmetry

It was very easy to find single crystal fragments suitable for X-ray diffraction work among the fragments of the crushed alloy sample. The crystal fragments were mounted on thin glass fibers with silicone grease in preparation for X-ray photography. From Laue photography it was established that the single crystal fragments were all of the same metallic phase and possessed Laue symmetry D_{6h}-6/mmm.

From the single crystal fragments rotation photographs with rotation about the a and c axes and Weissenberg photographs of the recipro-

---

*These amounts of silver and strontium do not correspond to the exact composition of Ag_4Sr. An excess of silver was used to make sure that if a second phase should appear, it would be the easily identified silver phase.

cal lattice nets with $\ell = 0, 1, 2$ and 3 and the net with $k = 0$ were taken with a Supper Weissenberg goniometer. These single crystal photographs were supplemented by a powder photograph taken with a Straumanis type camera. All of the photographs were taken with copper K_α radiation.*

C. Determination of the Unit Cell Dimensions

Approximate unit cell dimensions were obtained from the interlayer distances on the rotation photographs. They were found to be

$$a_o = 5.68 \text{ Å} ,$$
$$c_o = 4.60 \text{ Å} .$$

Since all of the diffraction arcs on the powder photograph could be indexed on the basis of a hexagonal cell with these cell dimensions, it was concluded that all or nearly all of the alloy sample consisted of one phase with a composition at least very close to the composition $Ag_{5.03}Sr$. The reported composition Ag_4Sr consequently appeared very unlikely.

For the accurate determination of the cell dimensions a least square refinement was made on the basis of powder data. The diffraction arcs were measured with a comparator with a precision of about 0.02 mm.

There were three parameters to be determined in the least squares

---

*The X-ray tubes were operated at a voltage of 25 KV to prevent the K-fluorescence of silver which was very serious when the X-ray tubes were operated at appreciably higher voltages. This method of reducing the fluorescence loses its usefulness for alloys richer in strontium since the K-fluorescence of the strontium is correspondingly stronger and its diminution requires the voltage applied across the X-ray tube to be less than 16.1 KV. Such low voltages are not practical because of the low intensity of the copper K_α radiation.

refinement, namely the radius of the camera and the lattice constants a_o and c_o. However, to simplify the refinement process the camera radius was determined separately by a least squares procedure.

For the least squares refinement of the lattice constants it was convenient to use the quantity Q given by the equation

$$Q = \frac{4 \sin^2 \theta}{\lambda^2} = \frac{4(h^2 + k^2 + hk)}{3a_o^2} + \frac{\ell^2}{c_o^2}$$

as the observed quantity. For the weighting of the observed quantities it was assumed that all the diffraction arcs could be measured with the same precision* and that systematic errors could be ignored. Thus, since dQ is proportional to sin 2θ dθ, the weight of the Q's could be taken to be $1/\sin^2 2\theta$.

The results of the least squares refinement of data obtained at 25° C. were

$$a_o = 5.681 \pm 0.001 \text{ Å} ,$$
$$c_o = 4.609 \pm 0.001 \text{ Å} ,$$

where the uncertainties are the probable errors.

Comparison of the uncertainties in a_o and c_o with those resulting from the uncertainty affecting the value of the radius of the camera showed that the latter was about one-tenth of the former. This fact justified the separate determination of the camera radius, and the probable errors are significant provided, of course, that the systematic errors are negligible.

---

*This is a suitable approximation since no powder lines were measured with θ > 80°.

In Table 1 are given the calculated and observed Q's, their differences and the corresponding weights. From the distribution of plus and minus signs in the last column it seems likely that small systematic errors such as absorption errors are present in the observed data. However, the magnitudes of the differences indicate that the systematic errors are not large enough to vitiate the significance of the results of the refinement.

D. The Unit Cell Contents and the Atomic Arrangement

The density of the alloy determined by the pycnometric method was 8.16 gm. cm.$^{-3}$. From this density the number of Ag_4Sr units per unit cell was found to be 1.20. This departure from an integral number is too large to be attributed to error in the density measurement alone. Since silver and strontium atoms are quite different in size, a disordered structure is improbable, and the only ordered structure compatible with the density and not in wild disagreement with the composition Ag_4Sr reported by Weibke contains one Ag_5Sr unit per unit cell. Calculation of the number of Ag_5Sr units per unit cell from the density gave the number 1.00. From this point on it was never questioned that the composition of the alloy is given by the formula Ag_5Sr.

The Weissenberg photographs did not show any systematic absences in the diffraction spectra. Therefore, the possible space groups were D_{6h}^1-P6/mmm, D_6^1-P622, C_{6v}^1-P6mm, D_{3h}^1-P$\bar{6}$m2 and D_{3h}^3-P$\bar{6}$2m .

At an early stage of the structure determination it was recognized that the Ag_5Sr phase probably has the already known $CaZn_5$ structure (3). Since there is no Strukturbericht designation for this type of structure

Table 1

The Observed and Calculated Q's

Index	Weight	Q_{obs}	Q_{calc}	$Q_{obs}-Q_{calc}$
100	10.42	0.0414	0.0413	0.0001
101	5.01	0.0886	0.0884	0.0002
110	3.30	0.1243	0.1240	0.0003
200	2.83	0.1649	0.1653	-0.0004
111	2.73	0.1716	0.1710	0.0006
002	2.51	0.1884	0.1883	0.0001
201	2.26	0.2128	0.2123	0.0005
102	2.13	0.2291	0.2296	-0.0005
210	1.76	0.2896	0.2892	0.0004
112	1.65	0.3126	0.3122	0.0004
211	1.56	0.3365	0.3363	0.0002
202	1.51	0.3531	0.3536	-0.0005
300	1.45	0.3719	0.3719	0.0000
301	1.34	0.4191	0.4189	0.0002
212	1.23	0.4778	0.4775	0.0003
220	1.20	0.4959	0.4958	0.0001
113	1.14	0.5473	0.5476	-0.0003
302	1.13	0.5601	0.5601	0.0000
203	1.10	0.5884	0.5889	-0.0005
400	1.05	0.6622	0.6611	0.0011
222	1.04	0.6842	0.6841	0.0001
401	1.03	0.7084	0.7081	0.0003

Table 1

The Observed and Calculated Q's
(Continued)

Index	Weight	Q_{obs}	Q_{calc}	$Q_{obs}-Q_{calc}$
312	1.02	0.7257	0.7254	0.0003
004	1.01	0.7532	0.7532	0.0000
303	1.00	0.7946	0.7955	-0.0009
411	1.01	0.9149	0.9147	0.0002
403	1.09	1.0823	1.0847	-0.0024
331	1.17	1.1600	1.1626	-0.0026
241_{α_1}	1.22	1.2043	1.2039	0.0004
224_{α_1}	1.30	1.2478	1.2490	-0.0012
224_{α_2}	1.32	1.2484	1.2490	-0.0006
314_{α_1}	1.39	1.2901	1.2903	-0.0002
314_{α_2}	1.41	1.2910	1.2903	0.0007
404_{α_1}	1.84	1.4129	1.4143	-0.0014
600_{α_1}	2.41	1.4874	1.4874	0.0000
333_{α_1}	3.14	1.5385	1.5392	-0.0007
333_{α_2}	3.30	1.5385	1.5392	-0.0007
423_{α_1}	4.26	1.5801	1.5805	-0.0004
423_{α_2}	4.59	1.5800	1.5805	-0.0005

it will be referred to here as the AB_5 structure. The structure has the space group D_{6h}^{1}-P6/mmm with the atoms in the following positions:

atom A in 1(a): 0,0,0;
atom B_1 in 2(c): 1/3,2/3,0; 2/3,1/3,0;
atom B_2 in 3(g): 1/2,0,1/2; 0,1/2,1/2; 1/2,1/2,1/2.

The conclusive evidence that the Ag_5Sr compound has the AB_5 structure came, of course, from the agreement between the calculated and observed diffraction intensities. Because the AB_5 structure has no parameters that need to be determined, semiquantitative intensity data were sufficient for establishing the AB_5 structure as the correct one. Table 2 contains the calculated intensities and the semiquantitative observed intensities. The agreement is reasonably good and establishes with certainty that the Ag_5Sr compound has the AB_5 structure.

The calculated intensities were obtained from the formula

$$I_{calc} = |F|^2 \left(\frac{1 + \cos^2 2\theta}{\sin 2\theta}\right) \left(1 - \frac{\sin^2 \beta}{\sin^2 \theta}\right)^{-1/2} A(\theta)$$

where F is the structure factor; θ is the Bragg angle; β is the Weissenberg equi-inclination angle; and $A(\theta)$ is the absorption factor. In calculating the absorption factor it was assumed that the crystal was cylindrical with a radius of 0.0125 cm. The linear absorption coefficient μ was calculated to be 1650. The form of $A(\theta)$ for non-zero layer Weissenberg data has been given by Miller (4). The structure factors were calculated using Thomas-Fermi atomic form factors modified to take into account the effect of anomalous dispersion upon both the K and L electrons in the silver and the strontium atoms. No temperature corrections were calculated since the absorption corrections

Table 2

The Calculated and Observed Intensities

Index	I_{calc}	I_{obs}
100	495	M
200	2230	MS
300	826	M
400	1860	S
500	535	MW
600	29,000	VS
110	895	M
210	503	MS
310	421	M
410	960	M
510	845	M
220	7600	S
320	396	MW
420	2856	S
520	5470	S
330	1050	M
430	1830	M
101	165	MW
201	2800	S
301	3320	S
401	2540	S
501	290	W
601	87	W
111	4160	S
211	160	MW
311	116	MW
411	3820	S
511	259	M
221	19	W
321	120	MW
421	4660	S
331	5260	S
431	785	M
102	292	M
202	1420	S
302	560	MS
402	1655	S
502	654	MW
112	538	M
212	338	M
312	325	M
412	880	M
512	1230	M
222	7080	VS
322	393	MW
422	4030	S
332	1390	M
103	59	W
203	1420	S
303	2230	S
403	2680	S
503	308	W
113	1640	MS
213	79	W
313	101	W
413	5640	S
223	15	W
323	151	W
423	12,300	S
333	12,300	S
001	21	VW
002	9650	VS
003	22	Absent
004	8160	VS
005	37	Absent

VS = very strong; S = strong; MS = medium strong; M = medium

MM = medium weak; W = weak; VW = very weak.

that were made were estimated to be much larger.

E. Discussion

The AB_5 structure is a well known structure (3,5,6,7 and 8) and need not be discussed in great detail, but it will be recalled that each A atom is surrounded by twenty nearest neighbors of which eighteen are B atoms (six B_1 and twelve B_2) and two are A atoms. The B atoms of both types are surrounded by twelve nearest neighbors. The B_1 atoms are surrounded by three A atoms and nine B atoms (three B_1 and six B_2) while the B_2 atoms are surrounded by four A atoms and eight B atoms (four B_1 and four B_2).

The different binary systems in which the AB_5 structure occurs are rather diverse. The only unifying features among them are the values of the radius ratio and the c_o/a_o ratio (Table 3). Undoubtedly the stability of the AB_5 structure can be attributed to the achievement of good packing when the radius ratio is in the range 0.632 to 0.709.

It is of interest to interpret the structural features of the Ag_5Sr compound in terms of the Pauling theory of bonding in metals (9). This theory relates the observed interatomic distances of two atoms to a bond number by the formula

$$D(1) - D(n) = 0.600 \log n$$

where D(1) is the sum of the single-bond radii of the two atoms involved in the bond, D(n) is the observed interatomic distance between the atoms and n is the bond number. Table 4 contains the interatomic distances of nearest neighbors and the corresponding bond numbers. The sum of the

Table 3

The Radius Ratios and c_o/a_o Ratios of Some AB_5 Compounds

Compound	Radius Ratio*	c_o/a_o
Ag_5Sr	0.670	1.23
Zn_5Ca (3),(5)	0.675	1.27, 1.29
Ni_5Ca (3)	0.632	1.25
Cu_5Ca (3),(5)	0.649	1.25, 1.24
Ni_5La (3)	0.664	1.23
Cu_5La (3)	0.683	1.25
Zn_5La (3)	0.709	1.28
Ni_5Ce (3),(6)	0.683	1.21
Co_5Ce (6)	0.690	---
Ni_5Gd (7)	0.698	1.23
Ni_5Pr (7)	0.683	1.24
Fe_5Th (8)	0.702	1.27
Co_5Th (8)	0.697	1.26
Ni_5Th (8)	0.692	1.23

*The radius ratios were computed using the metallic radii for coordination number 12(10).

bond numbers for the strontium atoms is 8.04 and for the silver atoms 6.49 and 5.31 for Ag_1 and Ag_2 respectively. As the metallic valences given by Pauling are 2.00 for strontium and 5.44 for silver, the values 8.04 and 6.49 are considerably too large. Only the sum 5.31 obtained for the Ag_2 atoms agrees well with the assigned valence. In considering a cause for the departure of these results from the expected values it is important to notice the remarkably high bond number (0.902) for the $Sr-Ag_1$ bond. Large bond numbers for this type of bond seem to be characteristic of all the AB_5 structures -- at least for all the compounds listed in Table 3 and is even greater than unity for the compound Ni_5Ca. Apparently the AB_5 structure achieves over-all good packing at the expense of compressing the $A-B_1$ bonds. Pauling points out that structures with strained bonds are exceptional and can not be expected to be interpreted simply (9).

Table 4

Interatomic Distances and the Corresponding Bond Numbers

Type of Bond	Length (Å)	Bond Number (n)
Sr-Sr	4.609	0.050
$Sr-Ag_1$	3.280	0.902
$Sr-Ag_2$	3.658	0.211
Ag_1-Ag_1	3.280	0.101
Ag_1-Ag_2	2.820	0.580
Ag_2-Ag_2	2.840	0.537

A remark about the composition assigned to this compound by Weibke should be made. His incorrect conclusion as to the chemical formula of the compound is not surprising since the composition of Ag_5Sr differs from that of Ag_4Sr by only 3% by weight and the method of thermal analysis which he used does not permit a very accurate determination of the composition of the intermetallic compounds formed.

III. THE INTERMETALLIC COMPOUND Ag_5Sr_3

A. Materials

An alloy of the approximate composition Ag_5Sr_3 was prepared from 13.44 gm. of silver and 6.56 gm. of strontium by the same method used in preparing the Ag_5Sr alloy and with metals from the same sources. The composition of a representative portion of the resulting alloy determined by chemical analysis agreed to within 1/2% with the formula Ag_5Sr_3.

The alloy was brittle and silvery in appearance. However, when exposed to air it soon tarnished to a deep yellow color.

B. X-ray Photography and Laue Symmetry

Of some twenty-five alloy fragments that were isolated from the crushed alloy sample and subsequently mounted and sealed in glass capillaries three were found to be single crystals upon investigation with the Laue goniometer. They were all of the same metallic phase and possessed Laue symmetry D_{2h}-mmm. From one of these crystals a rotation photograph with rotation about one of the orthorhombic axis, labeled the a_o axis, and Weissenberg photographs of the reciprocal lattice nets with h = 0,1,2,3,4,5,6 and 8 were obtained with a Supper Weissenberg goniometer using copper K_α radiation. Precession photographs of the reciprocal lattice nets with k = 0 and $\ell = 0$ were also obtained from this crystal with a Supper precession goniometer using molybdenum K_α radiation. Finally with a Philips powder camera (Straumanis arrangement) a powder photograph was obtained from a powder sample using copper K_α radiation. The sample was sealed in a glass capillary which had an inside diameter of about 0.1 mm.

C. The Unit Cell Dimensions

From measurements made on Weissenberg and rotation photographs the approximate unit cell dimensions were found to be

$$a_o = 9.6 \text{ Å} ,$$
$$b_o = 7.7 \text{ Å} ,$$
$$c_o = 16.5 \text{ Å} .$$

The diffraction pattern of the powder specimen was only moderately complicated. It was possible to index unambiguously all the measurable diffraction arcs* on the basis of the orthorhombic unit cell derived from single crystal data. The agreement between the semiquantitative powder intensities with the single crystal intensity data both facilitated the indexing of the diffraction arcs and provided a check of the correctness of the indices.

Because of the good agreement between the powder data and the single crystal data, it was concluded that the alloy sample consisted completely (or nearly completely) of the same phase as the single crystal fragments. As a consequence the single crystals must have a composition nearly corresponding to the formula Ag_5Sr_3.

To obtain more accurate cell dimensions a least squares refinement was carried out on the basis of the powder data. In order to

---

*There were about 70 to 75 diffraction arcs visible on the photograph and 62 of these were measurable on a comparator with a precision of about 0.02 mm. The background on the photograph due to the fluorescence of the powder specimen made it impossible to measure the remaining diffraction arcs which were all very weak and all occurred at Bragg angles greater than 40°. This latter group was not given any further consideration.

simplify the refinement the radius was determined separately by a least squares procedure. For the refinement of the three lattice constants it was convenient to use the quantity Q given by the equation

$$Q = \frac{4 \sin^2 \theta}{\lambda^2} = \frac{h^2}{a_o^2} + \frac{k^2}{b_o^2} + \frac{\ell^2}{c_o^2}$$

as the observed quantity.

The weights of the observations were chosen to be $1/\sin^2 2\theta$ since all the diffraction arcs could be measured with about the same precision. The diffraction arc 6.2.18 was an exception. It could not be measured as accurately as the other arcs because of line broadening as is generally the case for large Bragg angles and consequently was given only half the calculated weight.

The results of the refinement of the powder data obtained at 25° C. were

$$a_o = 9.619 \pm 0.002 \text{ Å} ,$$
$$b_o = 7.654 \pm 0.002 \text{ Å} ,$$
$$c_o = 16.555 \pm 0.007 \text{ Å} ,$$

where the uncertainties are the probable errors.

Table 5 lists the final values of the calculated and observed Q's along with their differences and the corresponding weights. There appears to be a slight trend in the distribution of positive and negative signs in the difference column indicating that there is very likely a small systematic error present in the experimental data. However, the effect of the systematic error was estimated and found to be sufficiently small that the values of the cell dimensions and their corresponding probable error retain their full significance.

Table 5

The Observed and Calculated Q's

Index	Weight	Q_{obs}	Q_{calc}	$Q_{obs} - Q_{calc}$
214	3.74	0.1203	0.1187	0.0016
024	3.55	0.1273	0.1267	0.0006
032	2.76	0.1684	0.1682	0.0002
400	2.67	0.1750	0.1729	0.0021
206	2.64	0.1764	0.1746	0.0018
226	2.01	0.2445	0.2429	0.0016
234	1.94	0.2559	0.2552	0.0007
040	1.84	0.2731	0.2731	0.0000
036	1.76	0.2870	0.2850	0.0020
028	1.70	0.3015	0.3018	-0.0003
044	1.57	0.3320	0.3315	0.0005
432	1.54	0.3421	0.3411	0.0010
0.1.10	1.41	0.3844	0.3820	0.0024
238	1.31	0.4315	0.4303	0.0012
440	1.28	0.4461	0.4460	0.0001
614	1.25	0.4657	0.4645	0.0012
622	1.24	0.4730	0.4719	0.0011
2.2.10	1.23	0.4770	0.4764	0.0006
0.0.12	1.16	0.5248	0.5254	-0.0006
4.1.10	1.13	0.5567	0.5549	0.0018
626	1.10	0.5887	0.5887	0.0000
634	1.09	0.6005	0.6010	-0.0005

Table 5

The Observed and Calculated Q's (Continued)

Index	Weight	Q_{obs}	Q_{calc}	$Q_{obs} - Q_{calc}$
060	1.08	0.6129	0.6145	-0.0016
800_{α_1}	1.03	0.6925	0.6915	0.0010
800_{α_2}	1.03	0.6910	0.6915	-0.0005
258_{α_1}	1.03	0.7032	0.7035	-0.0003
638_{α_1}	1.01	0.7762	0.7761	0.0001
638_{α_2}	1.00	0.7764	0.7761	0.0003
646_{α_1}	1.00	0.7923	0.7935	-0.0012
824_{α_1}	1.00	0.8190	0.8182	0.0008
824_{α_2}	1.00	0.8194	0.8182	0.0012
832_{α_1}	1.00	0.8605	0.8597	0.0008
832_{α_2}	1.00	0.8604	0.8597	0.0007
654_{α_1}	1.00	0.8725	0.8742	-0.0017
654_{α_2}	1.00	0.8728	0.8742	-0.0014
840_{α_1}	1.02	0.9645	0.9646	-0.0001
840_{α_2}	1.02	0.9648	0.9646	0.0002
828_{α_1}	1.04	0.9949	0.9944	0.0005
828_{α_2}	1.04	0.9946	0.9944	0.0002
$4.3.14_{\alpha_1}$	1.06	1.0437	1.0417	0.0020
$4.3.14_{\alpha_2}$	1.07	1.0432	1.0415	0.0015
$8.1.10_{\alpha_1}$	1.08	1.0723	1.0735	-0.0012
$8.1.10_{\alpha_2}$	1.09	1.0720	1.0735	-0.0015

Table 5

The Observed and Calculated Q's (Continued)

Index	Weight	Q_{obs}	Q_{calc}	$Q_{obs} - Q_{calc}$
$6.0.14_{\alpha_1}$	1.11	1.1049	1.1042	0.0007
$6.0.14_{\alpha_2}$	1.12	1.1050	1.1042	0.0008
666_{α_1}	1.14	1.1350	1.1349	0.0001
666_{α_2}	1.14	1.1344	1.1349	-0.0005
$10.0.6_{\alpha_1}$	1.24	1.2126	1.2119	0.0007
$10.0.6_{\alpha_2}$	1.25	1.2132	1.2119	0.0013
$2.2.18_{\alpha_1}$	1.41	1.2939	1.2938	0.0001
$2.7.12_{\alpha_1}$	1.79	1.4035	1.4050	-0.0015
$2.7.12_{\alpha_2}$	1.82	1.4038	1.4050	-0.0012
$0.0.20_{\alpha_1}$	2.20	1.4589	1.4596	-0.0007
$0.0.20_{\alpha_2}$	2.26	1.4593	1.4596	-0.0003
$6.3.16_{\alpha_1}$	2.33	1.4785	1.4767	0.0018
$6.3.16_{\alpha_2}$	2.39	1.4786	1.4767	0.0019
$0.7.14_{\alpha_1}$	3.46	1.5536	1.5516	0.0020
$12.0.0_{\alpha_1}$	3.62	1.5547	1.5559	-0.0012
$12.0.0_{\alpha_2}$	3.83	1.5554	1.5559	-0.0005
$6.2.18_{\alpha_1}$	8.72/2	1.6400	1.6396	-0.0004
$6.2.18_{\alpha_2}$	9.78/2	1.6391	1.6396	-0.0005

D. The Trial Structure

From the Weissenberg diffraction data the rules for the occurrence of reflections were found to be

$(hk\ell)$ all orders,
$(0k\ell)$ only with ℓ even,
$(h0\ell)$ only with h and ℓ even,
$(hk0)$ only with h and k even.

These rules do not uniquely determine a space group. The probable space groups are D_{2h}^{8}-Pcca and D_{2h}^{15}-Pbca.

There are a great many more absences in the diffraction data than are required by any of the possible space groups. These absences occur in a systematic way and their interpretation led directly to a trial structure. All the reflections on the reciprocal lattice nets with h odd were very weak. Ignoring all these weak reflections the remaining reflections (those with h even) could be re-indexed on the basis of an orthorhombic unit with the cell dimensions

$a_o' = a_o/2$,
$b_o' = b_o$,
$c_o' = c_o/2$.

When these reflections were re-indexed on the basis of the smaller cell, it was found that the occurrence of diffraction maxima obeyed the rules:

$(h'k'\ell')$ only with $h' + k' + \ell'$ even,
$(h'k'0)$ only with h' and k' even.

The probable space groups of the approximate orthorhombic structure are D_{2h}^{28}-Imma and C_{2v}^{22}-Ima2.

The reciprocal lattice net with $k' = 0$ possesses pseudohexagonal symmetry not only with respect to location of the reciprocal lattice points* but also with respect to the intensity distribution. Furthermore, there is a marked tendency on this net toward the appearance of only the reflections with $\ell' = 3n$. At this point the similarity of the structure to the C_{32} structure (11) became apparent. The C_{32} structure is hexagonal and has three atoms per unit cell (one of type A and two of type B). The space group of the C_{32} structure is D^1_{6h}-C6/mmm with

atom A in 1(a): 0,0,0 ;

atoms B in 2(d): 1/3,2/3,1/2; 2/3,1/3,1/2 .

Many of the qualitative features of the diffraction pattern can be explained on the basis of the C_{32} structure with the strontium atoms in the 1(a) positions and the silver atoms in the 2(d) positions and its hexagonal axis parallel to the b axis of the orthorhombic unit. The agreement is quite good for the reflections with $k' = 0$, and it is not bad for the other reflections with k' even and ℓ' small. However, some discrepances are apparent. The C_{32} structure requires the reflections with k' odd to be absent while in general they are observed although tending to be weak for small k'. There are other difficulties. In the C_{32} structure the A atoms form straight rows parallel to the hexagonal axis (orthorhombic b' axis in this case), but such an arrangement would bring the strontium atoms too close to one another (only 3.85 Å apart). Both of the unfavorable features of the C_{32} structure can be removed by staggering the rows of strontium atoms in the (100) plane. As a consequence the positions of the silver atoms are also ad-

---

*For the reflections to fall at the lattice points of a true hexagonal net the ratio c_0'/a_0' would have to be equal to $\sqrt{3}$. It actually has the value 1.72.

justed. The over-all packing is much improved as a result of these shifts, and the reflections with k' odd are no longer absent. This staggering results in a new structure that is orthorhombic with the cell dimensions

$$a_o' = a_o/2 \; ,$$
$$b_o' = b_o \; ,$$
$$c_o' = c_o/2 \; .$$

It has the space group D_{2h}^{28}-Imma. The approximate coordinates of the atoms determined from packing considerations are

Sr in 4(e): $(0,0,0;1/2,1/2,1/2) \pm 0,1/4,z$; with $z = 0.06$;

Ag in 8(h): $(0,0,0;1/2,1/2,1/2) \pm 0,y,z;\ 0,1/2 + y, \bar{z}$; with $y = 0.07$ and $z = 0.66$.

Table 6 contains the calculated and semiquantitative observed intensities of the $(0k\ell)$ reflections. The calculated intensities were obtained from the formula

$$I_{calc} = |F|^2 \left(\frac{1 + \cos^2 2\theta}{\sin 2\theta}\right)$$

where F is the structure factor computed from the trial structure and θ is the Bragg angle. The absorption and temperature factors were not included in the formula above because the calculations were only intended to establish qualitative relationships between the observed and calculated intensities. Although there is only rough agreement between the calculated and observed values, it seems reasonably certain that this trial structure based on the small orthorhombic pseudocell is closely related to the true structure.

Table 6

The Values of I_{obs} and I_{calc} for the Trial Structure

Index	I_{obs}	I_{calc}
012	MW	372
004	W	129
020	MS	302
024	S	874
016	MW	222
032	S	2200
008	MW	695
040	M	54
036	MW	294
028	M	202
044	W	125
0.1.10	M	515
052	M	248
048	VW	8
0.3.10	MW	223
0.0.12	MS	320
056	W	31
0.2.12	M	499
060	MS	588
064	W	6
0.1.14	VW	9
0.5.10	S	515
0.4.12	VW	72
068	Absent	120
072	MW	18
0.3.14	S	243
0.0.16	M	112
076	W	45
0.2.16	VW	24
080	MW	136
0.6.12	W	139
0.5.14	W	72
0.1.18	W	38
0.4.16	W	44
0.3.18	MW	29
0.0.20	S	750
0.2.20	W	58
0.6.16	M	220

The composition of the trial structure corresponds to the formula Ag_2Sr rather than the reported composition of Ag_5Sr_3. Because of the great difference in the sizes of the silver and strontium atoms, it is quite unlikely that this discrepancy can be accounted for by assuming that the true structure is obtained from the trial structure by replacing some of the silver atoms by strontium atoms. However, the discrepancy is only 4% by weight, and the inherent inaccuracy of the thermal analysis method used by Weibke in determining the composition Ag_5Sr_3 does not make an error of that magnitude unlikely. Additional evidence in favor of the composition Ag_2Sr comes from density considerations. The density of the trial structure was found by calculation to be 6.55 gm. $cm.^{-3}$. The observed density of an alloy of the composition Ag_2Sr* determined by pycnometric methods was 6.63 gm. $cm.^{-3}$. The calculated and observed densities agree to within 1.2% which is quite satisfactory.

The more difficult problem of establishing the difference between the true structure and the approximate structure of the deformed C_{32} type remains to be solved. No clues were found from inspection of the intensity data for reflections with h odd. Numerous structures produced by slightly deforming the approximate trial structure to give a structure with the correct unit cell size were investigated. However, none of these structures were as satisfactory as the trial structure from the point of view of packing nor did the intensities of the reflections calculated for these structures agree satisfactorily with the observed intensities.

---

*This alloy was prepared from 26.2 gm. of silver and 10.6 gm. of strontium by the method used for preparing the Ag_5Sr compound.

E. Discussion

It is not surprising that the Ag_2Sr phase does not have the undistorted C_{32} structure as the radius ratio of strontium and silver does not appear to be favorable. The radius ratio of strontium and silver is 1.49 which is definitely at the lower limit of what seems to be the permissible range for the C_{32} structures (Table 7). Although it is not surprising that a distortion should occur, the magnitude of the distortion is a little surprising. The pseudohexagonal cell of the Ag_2Sr structure has a c_o/a_o ratio of 0.80 while the range of ratios for the C_{32} structure appears to be 1.00 - 1.15 (Table 7). It is possible that the type of bonding in the C_{32} structure is an important factor in stabilizing this type of structure, too, because the C_{32} structure seems to occur most frequently in binary compounds containing members of the boron family.

The Ag_2Sr structure appears to be most closely related to the Zn_2Sr structure (12). This structure may also be described as a distorted C_{32} structure. Like the Ag_2Sr structure it has orthorhombic symmetry and has the same general arrangement of atoms in the unit cell as the orthorhombic pseudounit of the Ag_2Sr structure. In the Zn_2Sr structure the pseudohexagonal cell corresponding to a unit of the C_{32} structure has a c_o/a_o ratio of 0.84 which is only slightly higher than that for the Ag_2Sr structure.

The interatomic distances for the trial structure of the Ag_2Sr compound are given in Table 8. The distances on a whole indicate that the packing of the trial structure although acceptable can undoubtedly be expected to be much improved in the true structure.

Table 7

The c_o/a_o Ratios and the Radius Ratios of Some Compounds Having the C_{32} Structure

Compound	c_o/a_o	Radius Ratio
MgB_2 (13)	1.14	1.82
ZrB_2 (14)	1.11	1.81
AlB_2 (15)	1.08	1.63
NbB_2 (14)	1.07	1.63
TaB_2 (14)	1.06	1.63
TiB_2 (14)	1.06	1.65
CrB_2 (14)	1.03	1.43
MoB_2 (16)	1.02	1.55
$LaGa_2$ (17)	1.02	1.53
VB_2 (14)	1.02	1.50
$CaGa_2$ (17)	1.00	1.61
$CeGa_2$ (17)	1.00	1.49

Table 8

Interatomic Distances in the Trial Structure

Type	Length (Å)
Sr-Sr	3.99,3.92 4.80
Sr-Ag	3.53,3.32 3.60,3.36
Ag-Ag	2.82,2.84 2.78

IV. THE INTERMETALLIC COMPOUND AgSr

A. Materials

An alloy containing equal molar quantities of silver and strontium (6.59 gm. of silver and 5.34 gm. of strontium) was prepared by the same method and from the same materials used to prepare the Ag_5Sr compound. The composition of a representative sample of the alloy was determined by chemical analysis and agreed to within 1/2% with the composition AgSr. The method of analysis was the same as that used for the Ag_5Sr compound.

The alloy was silvery gray in appearance and very brittle. Upon exposure to the atmosphere it rapidly turned black and soon crumbled to a black powder.

B. X-ray Photography and Laue Symmetry

Fragments of the alloy considered suitable for X-ray photography were selected from a crushed portion of the alloy which was kept under dried kerosene. This arrangement was used to prevent the crushed alloy fragments from reacting with the air. The fragments chosen for further examination were dropped into glass capillaries filled with molten paraffin. The capillaries were then sealed.

No true single crystal fragments of this phase were ever obtained although more than three hundred fragments were examined with the Laue goniometer. The fragments were all polycrystalline, and the diffraction maxima frequently appeared as long streaks. However, two fragments were found that were fairly well suited for further work. Both of them consisted of two single crystals in very nearly parallel alignment as well as numerous much smaller crystallites. The collection of reliable diffraction data could be done fairly easily with these fragments.

Upon orientation on the Laue goniometer the two alloy fragments were found to have Laue symmetry D_{2h}-mmm. They were oriented with different crystallographic axes parallel to the axis of the goniometer. Rotation photographs about these axes (labeled the a and c axes) as well as Weissenberg photographs of the reciprocal lattice nets with h = 0,1,2,3 and 4 and the nets with ℓ = 0,1,2,3 and 4 were taken with a Supper Weissenberg goniometer. Copper K_α radiation was used. A precession photograph of the reciprocal lattice net with k = 0 was taken with a Supper precession goniometer using molybdenum K_α radiation. Several powder photographs were taken with a Philips powder camera (Straumanis type) using copper K_α radiation. A nickel filter was placed between the sample and the film rather than between the X-ray source and the sample as is usually done in an attempt to prevent fogging of the film by fluorescent radiation from the sample. The intensity of the fluorescent radiation was reduced in this way. Nevertheless, there was still a great deal of background on the photographs. Likewise, lowering the voltage applied across the X-ray tube to its practical limit* did not prove efficacious in reducing the fluorescent radiation to a level where the fogging it produced would not interfere with the interpretation of the photographs. A Straumanis type rotation photograph of the reciprocal lattice net with h = 0 was taken using unfiltered copper radiation from a gas tube. A quartz powder sample (200 mesh) was photographed on the same film using copper K_α radiation from

---

*See footnote page 4.

a gas tube. An additional rotation photograph with rotation about the a axis was obtained with a powder sample of sodium chloride photographed on the same film. Copper K_α radiation was used.

C. The Determination of the Unit Cell Dimensions

The approximate unit cell dimensions were obtained from the rotation and Weissenberg data. They were found to be

$$a_o = 16.4 \text{ Å} ,$$
$$b_o = 4.8 \text{ Å} ,$$
$$c_o = 6.4 \text{ Å} .$$

As there were very few diffraction arcs visible in the back reflection region of the powder photograph and none of them measurable with great accuracy because of the heavy background, single crystal data had to be used for the accurate determination of the cell dimensions. Although the powder photographs were not sufficiently good to serve as the basis for an accurate determination of the cell dimensions, they did supply the necessary evidence that the alloy sample consisted completely or nearly completely of the same phase as the single crystal fragments since all the diffraction arcs in the front reflection region of the powder photograph could be indexed on the basis of the information obtained from the single crystal data.

The lattice constants b_o and c_o were accurately determined from data obtained from the Straumanis type rotation photograph of the reciprocal lattice net with $h = 0$. The radius of the camera was determined separately by a least squares procedure. The many sharp diffraction arcs of quartz powder were particularly easy to measure and were of great value in determining the camera radius accurately. All the measurements were made with a comparator with a precision of about 0.02 mm. For the least squares refinement the quantity Q given by the equation

$$Q = \frac{4 \sin^2 \theta}{\lambda^2} = \frac{k^2}{b_o^2} + \frac{\ell^2}{c_o^2}$$

was used as the observed quantity. The weights of the observations were taken to be $1/\sin^2 2\theta$ as was done in the corresponding case of the Ag_5Sr compound.

The results of the least squares refinement based on data obtained at 25° C. were

$$b_o = 4.792 \pm 0.001 \text{ Å} ,$$
$$c_o = 6.392 \pm 0.002 \text{ Å} .$$

The uncertainties are probable errors. In Table 9 the calculated and observed Q's, their differences, and the corresponding weights are given. The distribution of plus and minus signs in the difference column indicates that there are systematic errors present in the experimental data. However, estimates of these systematic errors were no larger than the probable errors. The results are consequently significant except that the probable errors are possibly a little low.

The accurate determination of the lattice parameter a_o was based on measurements of the distances between equivalent spots on a rotation photograph with rotation about the a axis. This method was chosen because of lack of crystals in suitable orientation for other, better methods. As mentioned previously a powder sample of sodium chloride was photographed on the same film. This was done in order to obtain data for an accurate determination of the effective radius of the film.

Table 9

The Observed and Calculated Q's

Index	Weight	Q_{obs}	Q_{calc}	$Q_{obs} - Q_{calc}$
020_β	3.21	0.1754	0.1742	0.0012
020_α	2.68	0.1754	0.1742	0.0012
004_β	1.62	0.3938	0.3916	0.0022
004_α	1.40	0.3930	0.3916	0.0014
024_β	1.25	0.5675	0.5658	0.0017
024_α	1.12	0.5670	0.5658	0.0012
040_β	1.12	0.6954	0.6968	-0.0014
040_α	1.03	0.6967	0.6968	-0.0001
044_β	1.00	1.0889	1.0883	0.0006
044_{α_1}	1.09	1.0882	1.0883	-0.0001
044_{α_2}	1.10	1.0894	1.0883	0.0011
008_β	1.37	1.5670	1.5663	0.0007
060_β	1.37	1.5670	1.5677	-0.0007
028_β	1.89	1.7396	1.7405	-0.0009

Sodium chloride was chosen as the calibration substance since its lattice constant has been determined with great accuracy (18). All the measurements obtained from the photograph were made with a comparator with a precision of about 0.02 mm. The average value of the parameter a_o obtained from these measurements was

$$a_o = 16.48 \pm 0.02 \text{ Å} .$$

The uncertainty is the probable error. The data were obtained at 25° C.

The probable error of the parameter a_o is undoubtedly significant as the signs of the residuals seem to vary in a random fashion and, furthermore, do not tend to increase or decrease much with increasing sin θ. Figure 1 illustrates this point. It shows the variation of the values of a_o obtained from individual measurements as a function of sin θ. The poorer definition of the diffraction maxima as sin θ approaches unity is the cause for the slightly greater spread in the values of a_o in this region. The probable error affecting the determination of the camera radius was found to produce an effect on the parameter a_o that was negligible in comparison to the reported probable error.

D. The Trial Structure

1. Contents of the Unit Cell

It was not possible to measure the density of the individual single crystal fragments. The only experimental density obtainable was the density of a representative sample of the alloy. By pycnometric methods this density was found to be 5.32 gm. cm.$^{-3}$. Assuming the composition of the alloy to be AgSr the integral number of AgSr units per unit cell

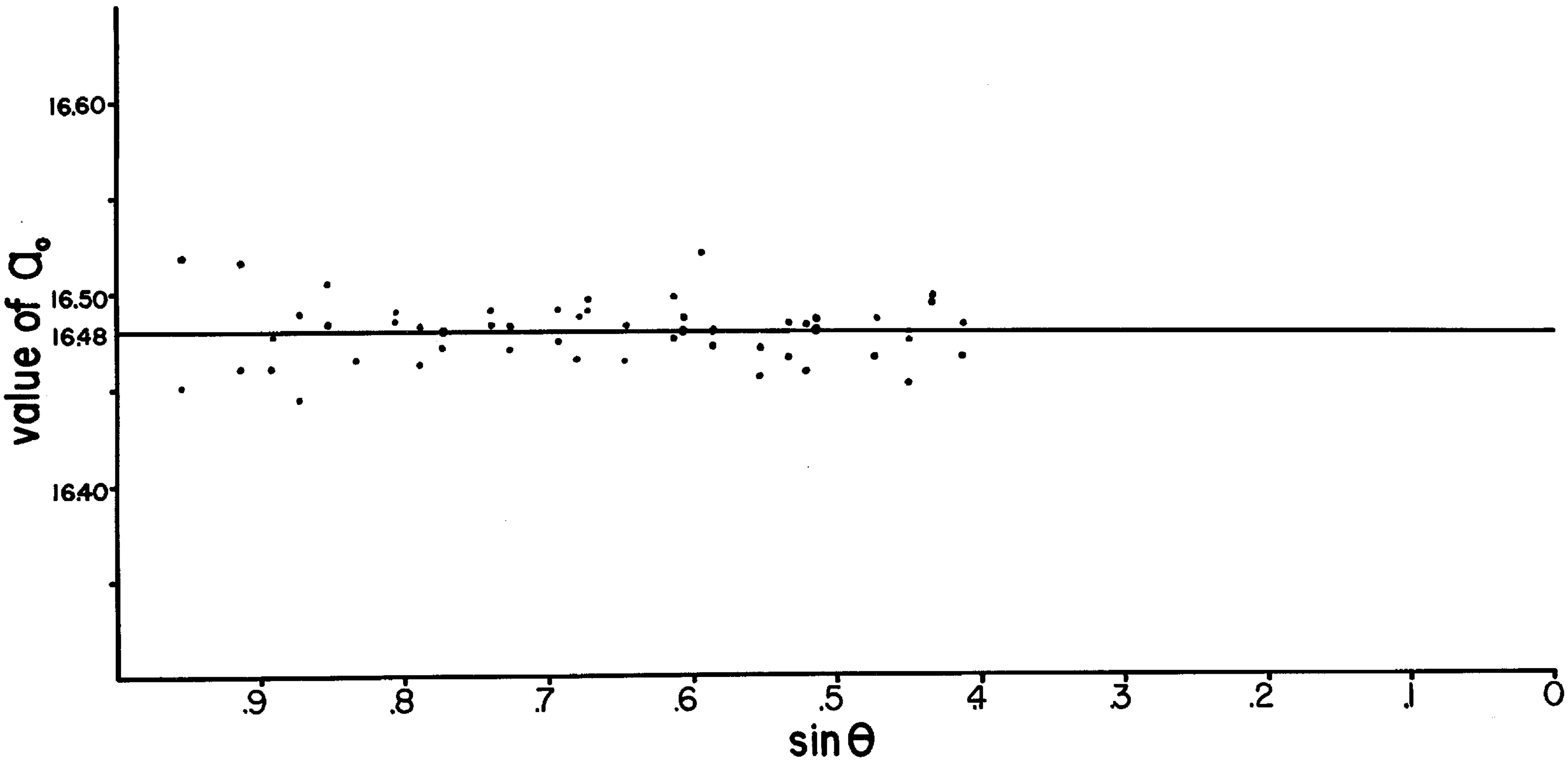

FIGURE I. A PLOT OF a_o AS A FUNCTION OF SIN θ that gives the best agreement between the calculated and observed density is eight. The calculated density is then 5.14 gm. cm.$^{-3}$. Although the agreement is not really good, it was tentatively assumed that there are eight AgSr units per unit cell. The justification for this assumption was primarily that the powder photograph did not indicate the presence of two phases in the alloy.

2. Positions of the Atoms

The following rules for the occurrence of reflections were established from the Weissenberg data:

$(hk\ell)$ all orders ,
$(h0\ell)$ all orders ,
$(hk0)$ only with $h = 4n$,
$(0k\ell)$ only with k even and $\ell = 4m$.

Not all of the absences can be space group extinctions. Nevertheless, on the basis of these absences the probable space groups could be shown to be D_{2h}^{16}-Pnma and C_{2v}^{9}-Pna2_1.

As the atomic scattering factors of silver and strontium do not differ greatly it was convenient to deduce a trial structure in which no distinction was made between the silver and strontium atoms. It then was possible to derive a trial structure from the purely qualitative features of the distribution of diffraction intensities. The following observations were made:

1. The observed reflections with ℓ odd and h small were much weaker than the reflections with ℓ even.
2. The paucity and the weakness of reflections with h odd was very pronounced.

3. There was a marked tendency among the (hk0) reflections toward the appearance of only those for which

   $h = 8m$ for k even,

   $h = 4 + 8n$ for k odd.

4. Among the $(0k\ell)$ reflections only those with k even and $\ell = 4n$ were observed.

5. The intensity distributions on the reciprocal lattice nets $\ell = 0$ and 4 were the same aside from normal decline. A similar situation occurred for the nets $\ell = 1$ and 3.

On the basis of the first and second observations it was concluded that to a fairly good approximation the structure has a pseudo unit cell with the dimensions

$$a_o' = a_o/2 \quad ,$$
$$b_o' = b_o \quad ,$$
$$c_o' = c_o/2.$$

This pseudo unit cell contains four atoms.

The third observation indicated that the projection of the true unit cell (and the pseudo unit cell) on the (001) plane has, to an approximation, a centered unit (Figure 2) with the dimensions

$$a_o'' = a_o/4 = a_o'/2 \quad ,$$
$$b_o'' = b_o = b_o' \ .$$

This fixes the x' and y' coordinates of the four atoms in the pseudo unit cell.

From the fourth observation it was deduced that the projection of the true unit cell (and the pseudo unit cell) on the (100) plane has a unit with the dimensions

$$b_o''' = b_o/2 = b_o'/2 \, ,$$
$$c_o''' = c_o/4 = c_o'/2 \, .$$

Thus the projection of the pseudo unit cell on the (100) plane has one atom per projected unit. Since there must be one atom per projected unit, no two atoms can have identical y' and z' coordinates in the pseudo unit cell. This determines the structure. If one of the atoms is placed arbitrarily at the origin of the pseudo unit cell then the coordinates of the atoms are

$x_1' = 0$, $x_2' = 1/2$, $x_3' = 1/4$, $x_4' = 3/4$,
$y_1' = 0$, $y_2' = 0$, $y_3' = 1/2$, $y_4' = 1/2$,
$z_1' = 0$, $z_2' = 1/2$, $z_3' = 0$ (or $1/2$), $z_4' = 1/2$ (or 0).

The two possibilities with respect to the choice of the z'-parameters, namely $z_3' = 0$ and $z_4' = 1/2$ or $z_3' = 1/2$ and $z_4' = 0$ do not represent different atomic arrangements and only one combination need be considered (Figure 3).

It may be noted that this assignment of z coordinates produces a layer structure with the layers being parallel to the (001) plane and separated by $c_o/4$. The fifth observation is a manifestation of this fact and supports the conclusions drawn from the first four observations.

An interesting feature of this arrangement becomes apparent if the unit cell is viewed down the b axis as shown in Figure 4. It is seen that the atoms lie at the lattice points of two somewhat deformed (stretched) hexagonal nets separated by the distance $b_o/2$ and that they are nearly in a close packed arrangement.

The trial structure derived in this section will hereafter be referred to as structure I.

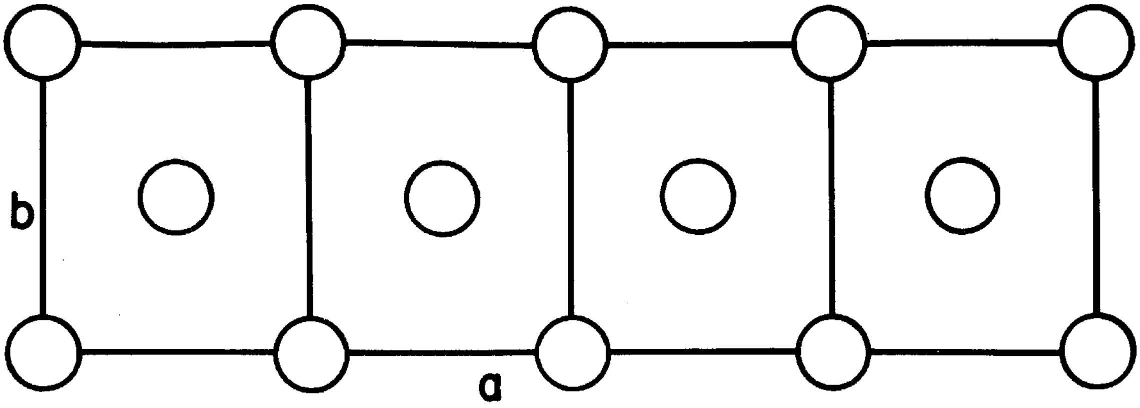

FIGURE 2. [C] PROJECTION

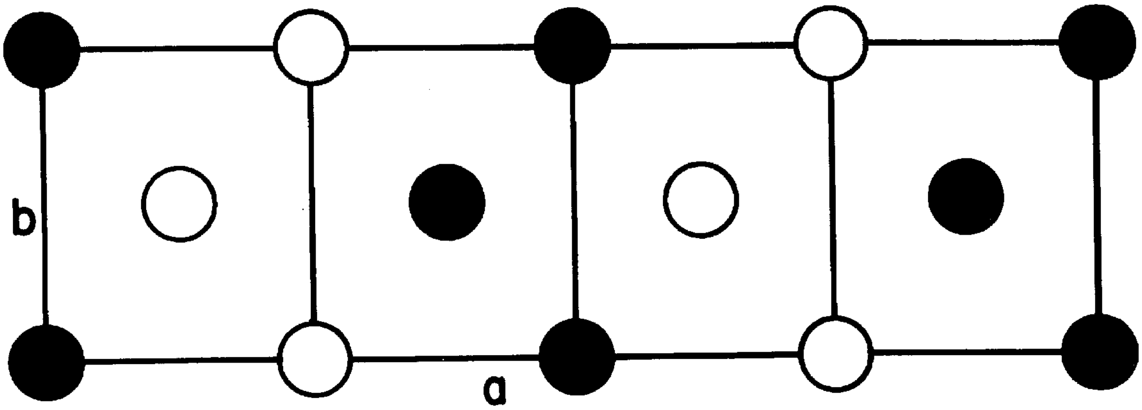

FIGURE 3.

[C] PROJECTION SHOWING THE Z PARAMETERS

○ $Z=0$ ($Z=0,\frac{1}{2}$ in true cell)

○ $Z=\frac{1}{2}$ ($Z=\frac{1}{4},\frac{3}{4}$ in true cell)

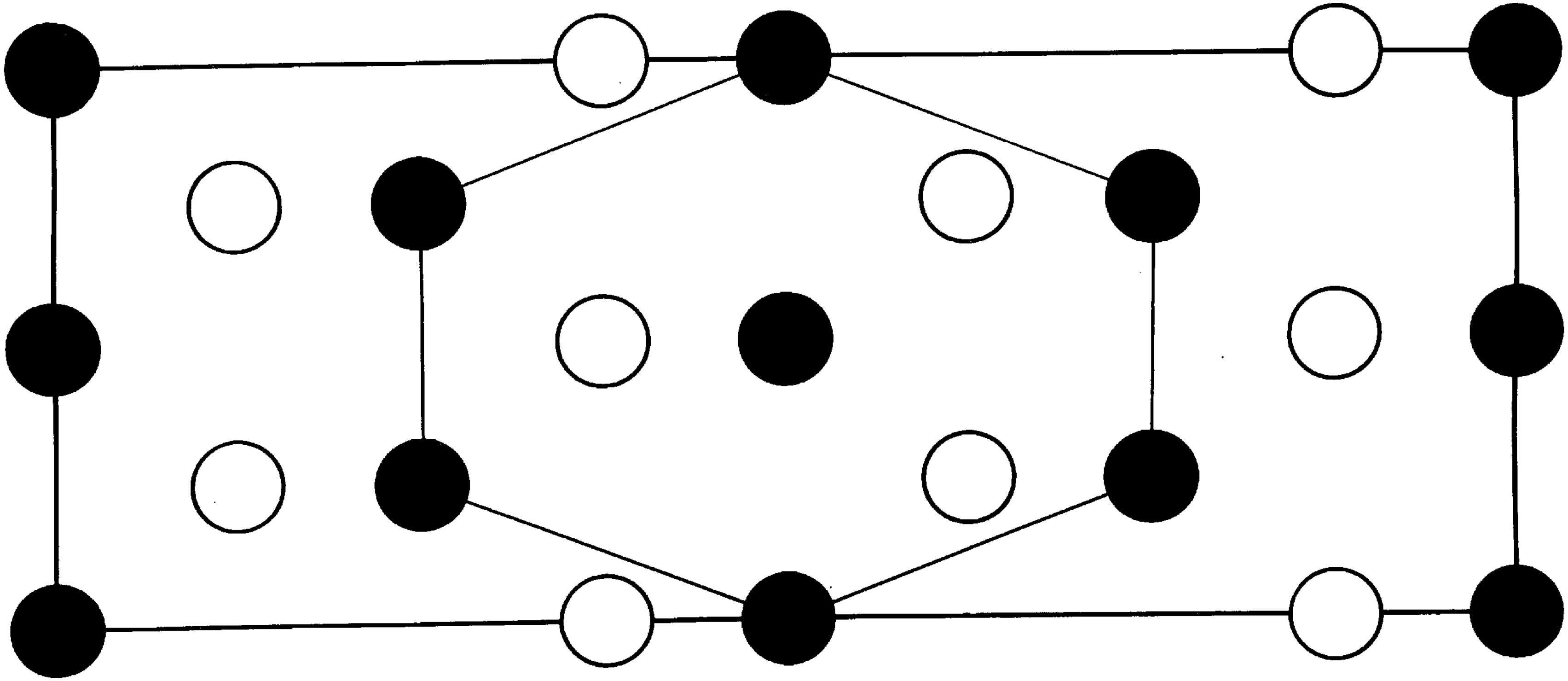

FIGURE 4. [b] PROJECTION OF THE UNIT CELL

● at Y=0 ○ at Y=$\frac{1}{2}$

3. Assignments of Silver and Strontium Positions

The metallic radii of silver and strontium differ sufficiently to make a disordered arrangement highly unlikely. Therefore it should be possible to specify the positions of the silver and strontium atoms in Structure I. This problem was solved in two steps. First, all the different arrangements of silver and strontium atoms at the lattice points of a stretched hexagonal net and with the correct unit cell size were derived. It was found that 28 different arrangements exist that are not related by a translation, a rotation or a combined translation and rotation (Figure 5).* Second, the different combinations of two of these nets (both identical or not and in every possible relative orientation with respect to each other) were investigated. Not all the possible combinations needed consideration. Only those leading to the composition AgSr and having a space group of orthorhombic symmetry with extinction rules compatible with the observed diffraction data were of any interest. There was a further restriction. The combinations possessing mirror planes that require neighboring strontium atoms to fall on straight lines parallel to the c axis could be excluded since the corresponding strontium-strontium distances (3.20 Å) would then be very much too short to be acceptable. The few remaining structures were improved by adjusting the positions of the atoms to

---

*Each stretched hexagonal net has eight different atomic sites. Each site is either occupied by a silver atom or it is not. Thus there are 2^8 or 256 possibly different arrangements but many of these are identical aside from a translation or a rotation or both. If the 28 different nets are each allowed to assume all orientations which lead to different arrangements of eight atoms, it is found that there are 256 such possibilities. This proves that these 28 nets exhaust all the different possibilities not related by rotations, translations or a combination of both of these operations.

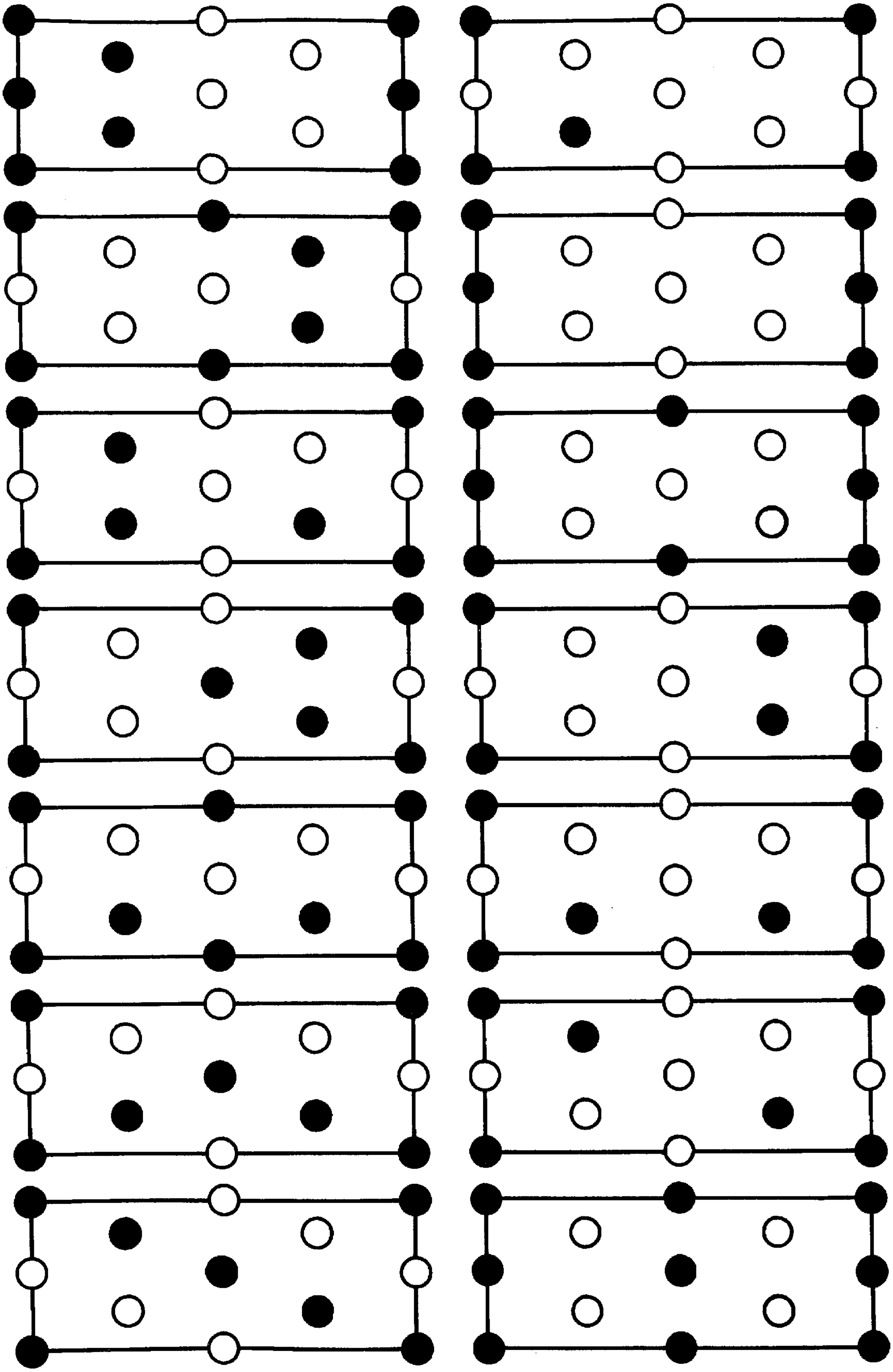

FIGURE 5. THE 28 POSSIBLE NETS

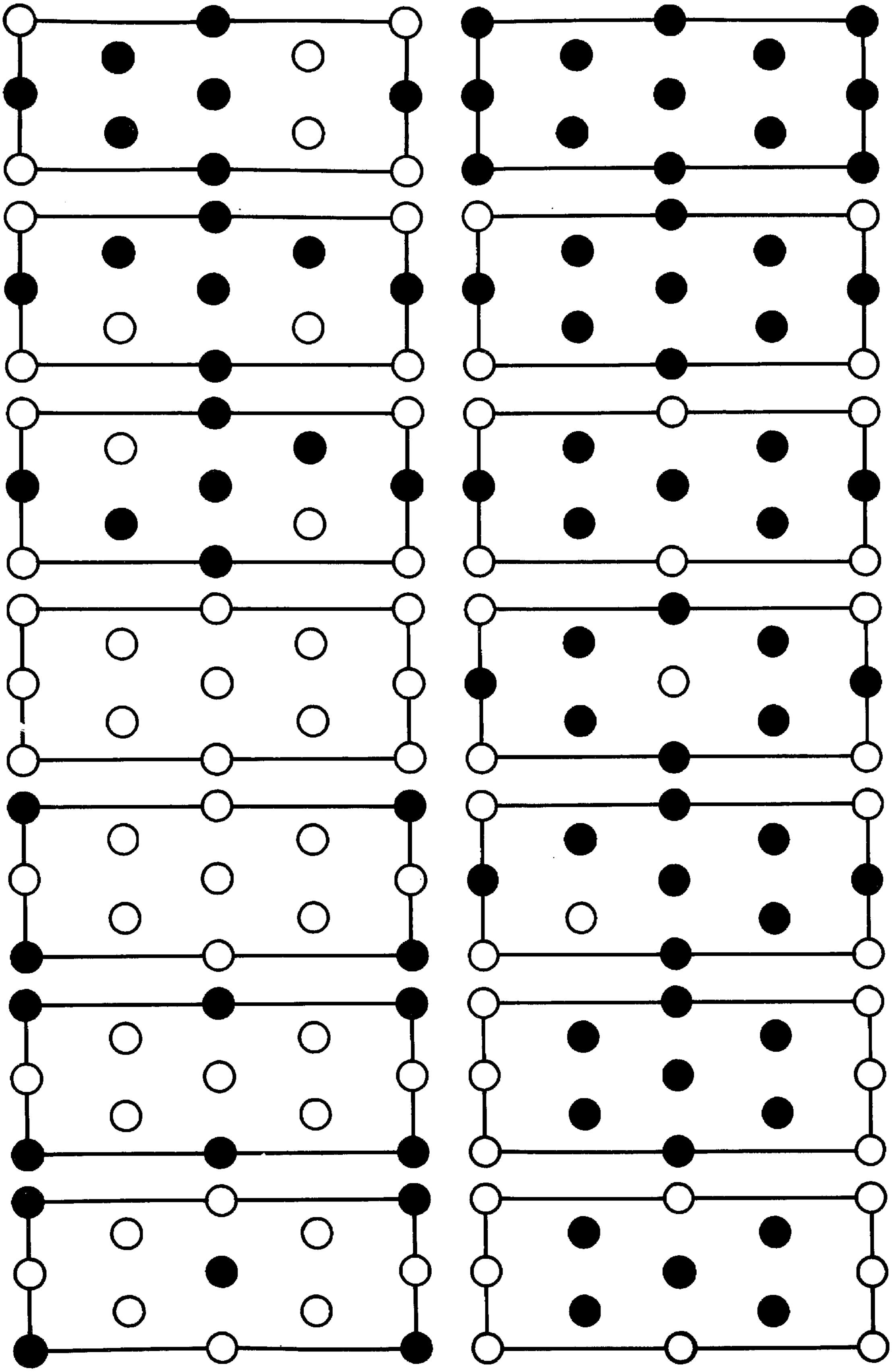

FIGURE 5 (continued).

● silver ○ strontium

get better over-all packing, but it was found that several very short strontium-strontium distances (c. 3.40 Å) could only be avoided in one of these structures. This one remaining structure required only very small displacements of the atoms from the positions of structure I to attain excellent over-all packing. This structure was adopted as the trial structure and will be referred to hereafter as structure II. Its space group is D_{2h}^{16}-Pnma, one of the probable space groups established earlier. The approximate positions of the atoms in the unit cell are

Sr_1 in 4(c): ± $(x, 1/4, z; 1/2+x, 1/4, 1/2-z)$ with $x_1=0.96$; $z_1=0.75$;
Sr_2 in 4(c): with $x_2=0.21$; $z_2=0.50$;
Ag_1 in 4(c): with $x_3=0.89$; $z_3=0.25$;
Ag_1 in 4(c): with $x_4=0.14$; $z_4=0.00$.

Structure II is shown in Figure 6. The two stretched hexagonal nets are pictured separately to illustrate how the strontium and silver atoms of one net fit into the large and small holes respectively in the neighboring nets.

In order to determine if structure II was a suitable trial structure a comparison of calculated and observed diffraction intensities was made. The calculated intensities were obtained with the use of the set of rough positional coordinates listed above. The Lorentz and polarization factors were taken into account but the temperature and absorption factors were ignored as this calculation was only meant to be qualitative. The agreement between the observed and calculated values was excellent not only for reflections with ℓ even but also for the generally weak reflections with ℓ odd. Therefore it was concluded that structure II was not only correct in its essential features but

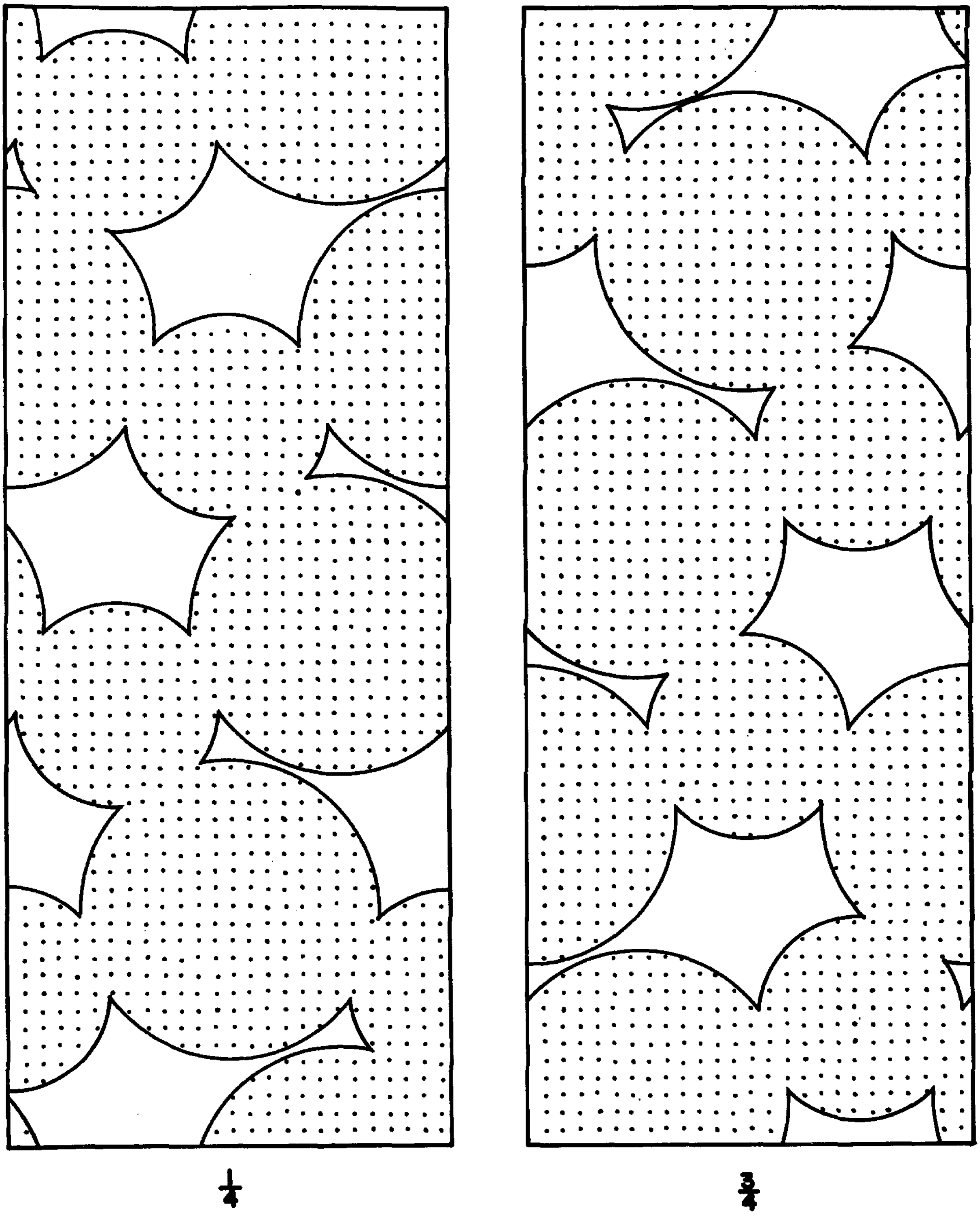

FIGURE 6.

LAYERS AT $Y=\frac{1}{4}$ AND $Y=\frac{3}{4}$

that the presumed rough coordinates were already close to the correct ones.

E. Refinement of Structure II

In spite of the success of structure II it was clear that it did not describe the true structure in every detail. The reciprocal lattice nets with ℓ odd showed pronounced streaks connecting lattice points with the same index k making it clear that the structure was disordered. The nature of this disorder will be discussed later. It was felt that before its details were established a refinement of all the positional parameters based on all the available data would not be worthwhile. The results might even be to some extent meaningless. Therefore a refinement of more limited scope was performed. It was assumed that the z-parameters were all exact multiples of 1/4 so that only the x-parameters required refinement.

Quantitative intensity data were obtained from Weissenberg photographs. The multiple film technique of de Lange, Robertson and Woodward was used (19). The intensities of the reflections were estimated visually by comparison with a standard intensity strip. The very strong reflections generally were only measured on the third film. The estimated intensities which were on a logarithmic scale were converted to a linear scale and multiplied by the appropriate film factors to reduce all of the intensities to the same scale. These reduced intensities, $I'(hk\ell)$, and the observed structure factors, $F(hk\ell)_{obs}$, were assumed to be related in the manner given by the equation

$$F(hk\ell)^2_{obs} = I'(hk\ell)P(\theta,\beta)Q^2(\sin\theta) \qquad (1)$$

where

$$P(\theta,\beta) = \left(\frac{\sin 2\theta}{1 + \cos^2 2\theta}\right)\left(1 - \frac{\sin^2 \beta}{\sin^2 \theta}\right)^{1/2} \quad ;$$

$Q^2(\sin\theta)$ is a combined scale, temperature and absorption factor;

θ is the Bragg angle;

β is the Weissenberg equi-inclination angle .

The nature of the function $Q(\sin\theta)$ had to be established. This was done in the usual way. The calculated structure factor, $|F(hk\ell)|_{calc}$ is approximately equal to $F(hk\ell)_{obs}$ and if substituted for the latter in equation (1) yields the equation

$$|F(hk\ell)|_{calc} / [I'(hk\ell)P(\theta,\beta)]^{1/2} = Q(\sin\theta). \tag{2}$$

To obtain $Q(\sin\theta)$ the related ratio

$$\sum |F(hk\ell)|_{calc} / \sum [I'(hk\ell)P(\theta,\beta)]^{1/2}$$

was preferred in order to reduce the effects of random fluctuations. It was plotted as a function of $\sin\theta$ for all the observable (hk0) reflections with the summations over ranges of the magnitude 1/10 (Figure 7). As the plot indicates, $Q(\sin\theta)$ is nearly constant over the whole range of $\sin\theta$ values. This undoubtedly means that the opposing effects of absorption and thermal vibrations very nearly cancel each other. Bradley has pointed out that in such cases it is justifiable to ignore both effects (20). This was done in the present case and $Q(\sin\theta)$ simply became a scale factor. The scale factors for the reciprocal lattice nets with $\ell = 1,2,3$ and 4 were obtained in the usual way by utilizing the intensity data of the nets with h = 0,1,2, etc.

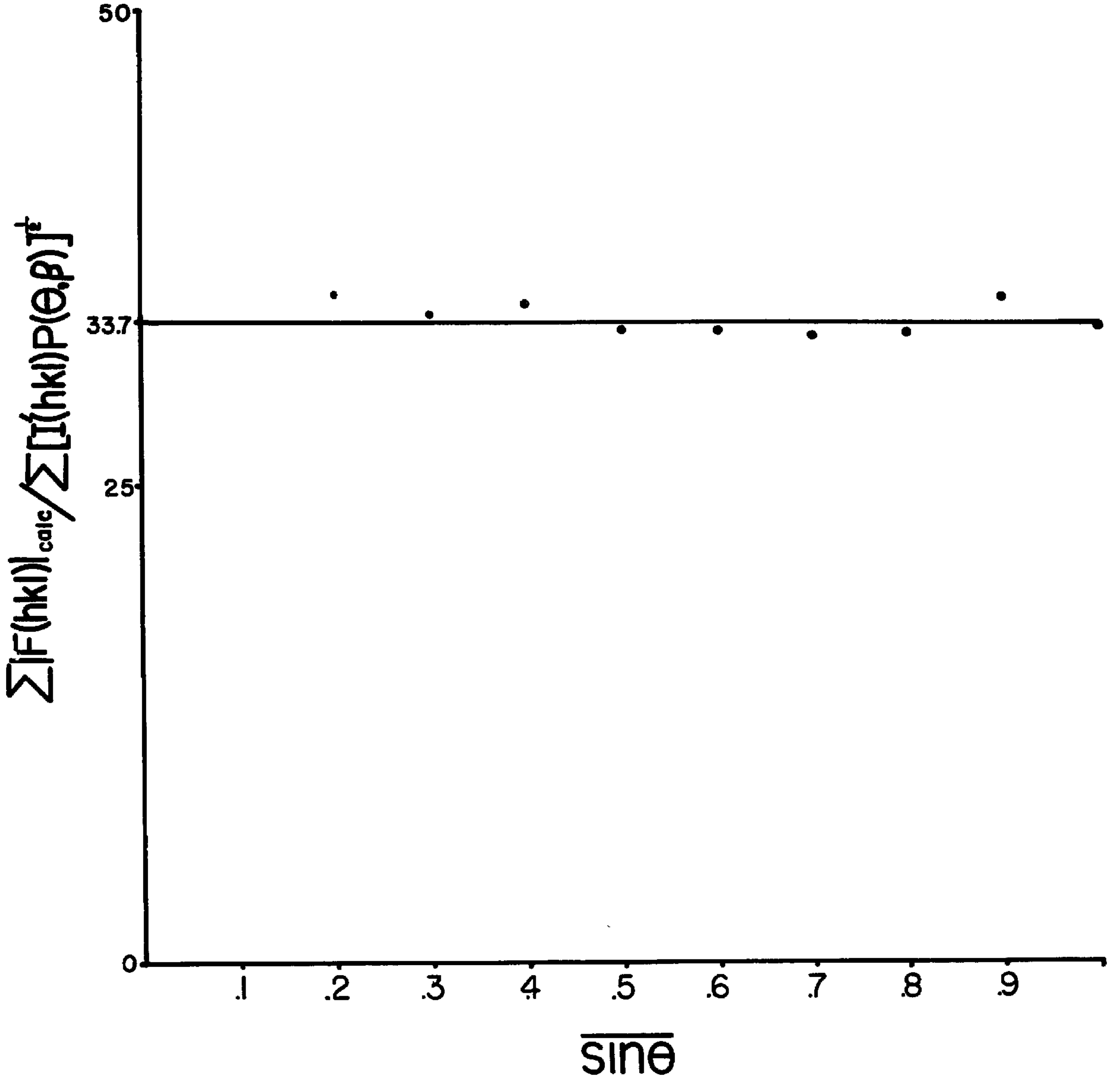

FIGURE 7.

DETERMINATION OF Q(sinθ) FOR THE (hkO) RECIPROCAL LATTICE NET to establish the necessary cross correlations.

The least squares refinement of the x-parameters was made on the basis of only the (hk0) data since the intensities of these reflections only depend on the x-parameters. To simplify matters the observed structure factors were all given the same weight. The results of the refinement were

$$x_1 = 0.963 \pm 0.002 \text{ Å} ,$$
$$x_2 = 0.214 \pm 0.002 \text{ Å} ,$$
$$x_3 = 0.892 \pm 0.002 \text{ Å} ,$$
$$x_4 = 0.140 \pm 0.002 \text{ Å} .$$

The uncertainties are the probable errors. The calculated structure factors for the refined set of x-parameters are given in Table 10 together with the observed structure factors and corresponding residuals. For reflections too weak to be observed a value corresponding to the minimum observable intensity has been recorded in the column for the observed structure factors preceded by the symbol < . On the whole the agreement between the calculated and observed structure factors is satisfactory. The reliability factor, R factor, defined by the formula

$$R = \sum \left| F(hk\ell)_{obs} - |F(hk\ell)|_{calc} \right| / \sum F(hk\ell)_{obs}$$

where the summation is over all the observed reflections was 0.140. However, a closer inspection of Table 10 reveals that while the agreement is excellent on the reciprocal lattice nets with ℓ even, the agreement on the nets with ℓ odd is only moderately good with a tendency for the observed reflections with h odd to be too low and with h even to be too high. This peculiarity is clearly reflected in the R factors of the individual reciprocal lattice nets (Table 11). Table 11

Table 10

Index	$\lvert F(hk\ell)\rvert_{calc}$	$F(hk\ell)_{obs}$	$\lvert\Delta F\rvert$	Index	$\lvert F(hk\ell)\rvert_{calc}$	$F(hk\ell)_{obs}$	$\lvert\Delta F\rvert$
200	0.0	<23		040	361.8	467	105.2
400	146.4	152	5.6	240	0.0	<74	
600	0.0	<42		440	95.2	93	2.2
800	135.0	126	9.0	640	0.0	<76	
10.0.0	0.0	<59		840	95.2	93	2.2
12.0.0	217.6	240	22.4	10.4.0	0.0	<72	
14.0.0	0.0	<74		12.4.0	170.4	179	8.6
16.0.0	142.2	150	7.8	14.4.0	0.0	<76	
18.0.0	0.0	<67		16.4.0	120.0	105	15
20.0.0	64.0	61	3	250	0.0	<70	
210	0.0	<34		450	175.2	186	10.8
410	316.0	327	11	650	0.0	<65	
610	0.0	<46		850	10.4	<58	
810	9.6	<54		10.5.0	0.0	<50	
10.1.0	0.0	<62		12.5.0	204.0	173	31
12.1.0	275.2	291	15.8	060	284.0	281	3
14.1.0	0.0	<75		260	0.0	<39	
16.1.0	255.2	227	28.2	460	78.4	85	6.6
18.1.0	0.0	<65		301	68.4	74	5.6
20.1.0	27.2	<46		401	31.6	<34	
020	508.8	487	21.8	501	145.6	116	29.6
220	0.0	<47		601	228.8	230	1.2
420	128.0	139	11	701	245.6	201	44.6
620	0.0	<56		801	196.4	250	53.6
820	120.0	126	6	901	10.4	88	16
10.2.0	0.0	<69		10.0.1	6.8	<60	
12.2.0	203.2	213	9.8	11.0.1	58.1	<65	
14.2.0	0.0	<75		12.0.1	73.6	70	3.6
16.2.0	135.2	129	6.2	13.0.1	43.2	<72	
18.2.0	0.0	<57		14.0.1	8.4	<74	
230	0.0	<62		15.0.1	51.2	<75	
430	230.4	227	3.4	16.0.1	63.2	76	12.8
630	0.0	<68		17.0.1	34.4	<70	
830	8.8	<72		18.0.1	23.6	<65	
10.3.0	0.0	<75		19.0.1	87.2	80	7.2
12.3.0	249.2	213	36.2	20.0.1	132.4	130	2.4
14.3.0	0.0	<70		21.0.1	139.2	140	.8
16.3.0	232.8	193	39.8	111	5.2	<32	

Table 10
(Continued)

Index	$\|F(hk\ell)\|_{calc}$	$F(hk\ell)_{obs}$	$\|\Delta F\|$	Index	$\|F(hk\ell)\|_{calc}$	$F(hk\ell)_{obs}$	$\|\Delta F\|$
211	76.8	90	13.2	031	33.2	<62	
311	164.4	166	1.6	131	8.4	<62	
411	210.8	226	15.2	231	52.8	110	57.2
511	188.8	170	18.8	331	120.4	130	9.6
611	105.2	108	2.8	431	159.2	200	40.8
711	8.8	<51		531	146.4	139	7.4
811	108.8	128	19.2	631	83.2	130	46.8
911	164.8	144	20.8	731	7.2	<71	
10.1.1	159.2	188	28.8	831	90.8	152	61.2
11.1.1	107.2	104	3.2	931	137.2	132	5.2
12.1.1	38.4	<70		10.3.1	135.2	152	16.8
13.1.1	13.6	<73		11.3.1	92.0	104	12.0
14.1.1	26.8	<75		12.3.1	33.6	<75	
15.1.1	.8	<75		13.3.1	13.2	<72	
16.1.1	50.0	88	38	14.3.1	26.4	<69	
17.1.1	98.8	82	16.8	15.3.1	3.2	<64	
18.1.1	119.6	140	20.4	16.3.1	44.8	68	23.2
19.1.1	104.4	80	24.4	17.3.1	91.6	66	25.6
20.1.1	52.4	72	19.6	18.3.1	111.6	113	1.4
121	65.2	100	34.8	141	48.4	<74	
221	92.0	151	59	241	68.0	100	32
321	58.8	58	.8	341	44.4	<75	
421	23.6	<52		441	16.8	<75	
521	122.0	124	2	541	92.4	100	7.6
621	195.6	222	26.4	641	150.0	197	47
721	214.0	200	14	741	168.0	160	8
821	173.6	192	18.4	841	138.8	185	46.2
921	92.4	78	14.4	941	74.8	83	8.2
10.2.1	6.0	<69		10.4.1	3.6	<70	
11.2.1	53.2	<72		11.4.1	46.0	<67	
12.2.1	67.2	<74		12.4.1	60.0	70	10
13.2.1	40.4	<75		13.4.1	36.4	<58	
14.2.1	7.6	<75		14.4.1	6.8	<52	
15.2.1	49.2	<73		15.4.1	43.2	<43	43.2
16.2.1	60.8	<69		051	27.2	<70	
17.2.1	34.0	<63		151	8.4	<70	
18.2.1	22.4	<56		251	39.6	<69	
19.2.1	85.2	80	5.2	351	92.0	100	8

Table 10
(Continued)

Index	$\|F(hk\ell)\|_{calc}$	$F(hk\ell)_{obs}$	$\|\Delta F\|$	Index	$\|F(hk\ell)\|_{calc}$	$F(hk\ell)_{obs}$	$\|\Delta F\|$
451	122.4	190	67.6	12.1.2	0.0	<69	
551	113.6	112	1.6	13.1.2	0.0	<71	
651	65.6	97	31.4	14.1.2	25.6	<72	
751	6.0	<61		15.1.2	0.0	<71	
851	73.2	100	26.8	16.1.2	0.0	<69	
951	112.4	124	11.6	17.1.2	0.0	<64	
10.5.1	112.0	140	28	18.1.2	153.6	139	14.6
11.5.1	79.2	66	13.2	19.1.2	0.0	<48	
12.5.1	28.0	<32		022	0.0	<43	
202	276.0	182	94	122	0.0	<43	
302	0.0	<28		222	230.4	232	1.6
402	0.0	<32		322	0.0	<50	
502	0.0	<38		422	0.0	<52	
602	120.0	130	10	522	0.0	<55	
702	0.0	<48		622	107.2	111	3.8
802	0.0	<52		722	0.0	<59	
902	0.0	<56		822	0.0	<62	
10.0.2	92.8	75	17.8	922	0.0	<65	
11.0.2	0.0	<64		10.2.2	86.4	90	3.6
12.0.2	0.0	<68		11.2.2	0.0	<71	
13.0.2	0.0	<71		12.2.2	0.0	<72	
14.0.2	341.6	328	13.6	13.2.2	0.0	<72	
15.0.2	0.0	<72		14.2.2	325.6	320	5.6
16.0.2	0.0	<70		15.2.2	0.0	<68	
17.0.2	0.0	<66		16.2.2	0.0	<63	
18.0.2	96.0	74	22	17.2.2	0.0	<57	
19.0.2	0.0	<51		18.2.2	92.0	<49	92
112	0.0	<30		132	0	<62	
212	387.2	397	9.8	232	299.2	323	23.8
312	0.0	<37		332	0.0	<64	
412	0.0	<40		432	0.0	<65	
512	0.0	<44		532	0.0	<66	
612	24.8	<47		632	21.6	<68	
712	0.0	<51		732	0.0	<69	
812	0.0	<55		832	0.0	<70	
912	0.0	<59		932	0.0	<72	
10.1.2	242.4	255	12.6	10.3.2	208.8	208	.8
11.1.2	0.0	<66		11.3.2	0	<72	

Table 10
(Continued)

Index	$\|F(hk\ell)\|_{calc}$	$F(hk\ell)_{obs}$	$\|\Delta F\|$	Index	$\|F(hk\ell)\|_{calc}$	$F(hk\ell)_{obs}$	$\|\Delta F\|$
12.3.2	0.0	<70		803	171.2	200	28.8
13.3.2	0.0	<67		903	91.6	108	16.4
14.3.2	23.2	<64		10.0.3	5.6	<63	
15.3.2	0.0	<58		11.0.3	52.8	<67	
16.3.2	0.0	<51		12.0.3	67.2	68	.8
17.3.2	0.0	<41		13.0.3	40.4	<70	
042	0.0	<72		14.0.3	7.6	<70	
142	0.0	<72		15.0.3	49.2	<68	
242	172.8	210	37.2	16.0.3	60.4	63	2.6
342	0.0	<72		17.0.3	33.6	<59	
442	0.0	<72		18.0.3	22.4	<52	
542	0.0	<72		19.0.3	84.8	80	4.8
642	85.6	109	23.4	013	35.2	34	1.2
742	0.0	<71		113	8.0	<35	
842	0.0	<70		213	60.4	82	21.6
942	0.0	<66		313	134.0	114	20
10.4.2	75.2	89	13.8	413	175.6	180	4.4
11.4.2	0.0	<62		513	160.4	145	15.4
12.4.2	0.0	<58		613	90.4	107	16.6
13.4.2	0.0	<52		713	8.0	<54	
14.4.2	286.4	274	12.4	813	97.6	113	15.4
152	0.0	<64		913	146.8	133	13.8
252	232.8	284	51.2	10.1.3	144.0	192	48
352	0.0	<63		11.1.3	97.2	67	30.2
452	0.0	<62		12.1.3	36.0	<70	
552	0.0	<60		13.1.3	12.4	<70	
652	23.2	<58		14.1.3	26.4	<70	
752	0.0	<55		15.1.3	2.4	<67	
852	0.0	<52		16.1.3	46.8	<63	
952	0.0	<47		17.1.3	94.0	80	14
10.5.2	175.2	175	.2	18.1.3	116.4	118	1.6
062	0.0	<24		19.1.3	100.4	84	16.4
203	89.6	67	22.6	123	57.2	56	1.2
303	57.2	53	4.5	223	80.4	135	54.6
403	23.2	<37		323	56.4	60	3.6
503	120.0	94	26	423	19.2	<55	
603	192.4	230	37.6	523	106.0	99	7
703	211.2	211	.2	623	171.2	220	48.8

Table 10
(Continued)

Index	$\lvert F(hk\ell)\rvert_{calc}$	$F(hk\ell)_{obs}$	$\lvert\Delta F\rvert$
723	190.4	165	25.4
823	156.0	177	21
923	84.0	77	7
10.2.3	5.6	<69	
11.2.3	49.6	<70	
12.2.3	64.0	69	5
13.2.3	38.4	<69	
14.2.3	7.2	<66	
15.2.3	47.2	<62	
16.2.3	58.4	55	3.4
17.2.3	32.4	<49	
18.2.3	22.0	<38	
033	31.2	64	32.8
133	8.4	<64	
233	47.6	124	76.4
333	108.8	112	3.2
433	144.0	210	66
533	132.8	142	9.2
633	75.2	147	71.8
733	6.4	<70	
833	82.8	100	17.2
933	128.0	135	7
10.3.3	126.8	165	38.2
11.3.3	86.8	77	9.8
12.3.3	30.4	<65	
13.3.3	13.6	<62	
14.3.3	26.0	<57	
15.3.3	2.4	<50	
16.3.3	43.6	41	2.6
143	45.6	<70	
243	64.0	110	46
343	42.0	<70	
443	15.2	<70	
543	86.0	81	5
643	140.8	230	89.2
743	157.6	155	2.6
843	130.4	170	39.6
943	70.0	81	11
10.4.3	3.2	<60	
11.4.3	45.2	<55	
12.4.3	56.8	61	4.2
13.4.3	34.0	<43	
14.4.3	6.4	<30	
053	26.8	<58	
153	8.8	<58	
253	36.8	90	53.2
353	87.6	87	.6
453	117.2	140	22.8
553	109.2	101	8.2
653	62.4	96	33.6
753	5.6	<46	
853	70.4	81	10.6
953	108.0	96	12
10.0.4	0.0	<62	
11.0.4	0.0	<63	
12.0.4	188.0	183	5
13.0.4	0.0	<64	
14.0.4	0.0	<62	
15.0.4	0.0	<58	
16.0.4	126.4	127	.6
17.0.4	0.0	<46	
114	0.0	<35	
214	0.0	<38	
314	0.0	<41	
414	226.4	192	34.4
514	0.0	<48	
614	0.0	<51	
714	0.0	<55	
814	8.8	<58	
914	0.0	<60	
10.1.4	0.0	<62	
11.1.4	0.0	<63	
12.1.4	238.4	237	1.4
13.1.4	0.0	<63	
14.1.4	0.0	<60	
15.1.4	0.0	<57	

Table 10
(Continued)

Index	$\vert F(hk\ell)\vert_{calc}$	$F(hk\ell)_{obs}$	$\vert\Delta F\vert$
16.1.4	229.6	184	45.6
17.1.4	0.0	<43	
024	384.0	400	16
124	0.0	<51	
224	0.0	<52	
324	0.0	<54	
424	102.4	102	.4
524	0.0	<57	
624	0.0	<59	
724	0.0	<61	
824	99.2	107	7.8
924	0.0	<64	
10.2.4	0.0	<64	
11.2.4	0.0	<64	
12.2.4	177.6	178	.4
13.2.4	0.0	<60	
14.2.4	0.0	<56	
15.2.4	0.0	<50	
16.2.4	123.2	126	2.8
134	0.0	<60	
234	0.0	<62	
334	0.0	<63	
434	192.8	258	65.2
534	0.0	<64	
634	0.0	<64	
734	0.0	<64	
834	9.6	<64	
934	0.0	<63	
10.3.4	0.0	<61	
11.3.4	0.0	<58	
12.3.4	217.6	220	2.4
13.3.4	0.0	<49	
14.3.4	0.0	<43	
044	318.4	360	41.6
144	0.0	<62	
244	0.0	<62	
344	0.0	<62	
444	87.2	98	10.8
544	0.0	<60	
644	0.0	<59	
744	0.0	<57	
844	88.0	95	7
944	0.0	<51	
10.4.4	0.0	<47	
11.4.4	0.0	<41	
12.4.4	158.4	127	31.4
154	0.0	<44	
254	0.0	<43	
354	0.0	<42	
454	162.4	162	.4
554	0.0	<34	

also provides a check that the assumption that the z-parameters are very nearly multiples of 1/4 was very good since the R factor of the (hk4) data is essentially as good as that of the (hk0) data.

Table 11

The R-Factors of the Individual Reciprocal Lattice Nets

Net	R-Factor
(hk0)	0.085
(hk1)	0.170
(hk2)	0.115
(hk3)	0.184
(hk4)	0.087

F. The Complete Interpretation of the Reciprocal Lattice Nets with ℓ odd

In the preceding section it was pointed out that the reciprocal lattice nets with ℓ odd were distinguished from the nets with ℓ even by much larger R factors. There was another distinguishing characteristic. The diffraction maxima on these nets although otherwise well defined had tails which connected neighboring maxima with the same k index. These tails were relatively more intense where the corresponding maxima were strong than elsewhere. Such spreading out of the diffraction maxima did not occur on the nets with ℓ even. Weissenberg photographs of the nets with ℓ = 2 and 3 have been reproduced in Figure 8 to show

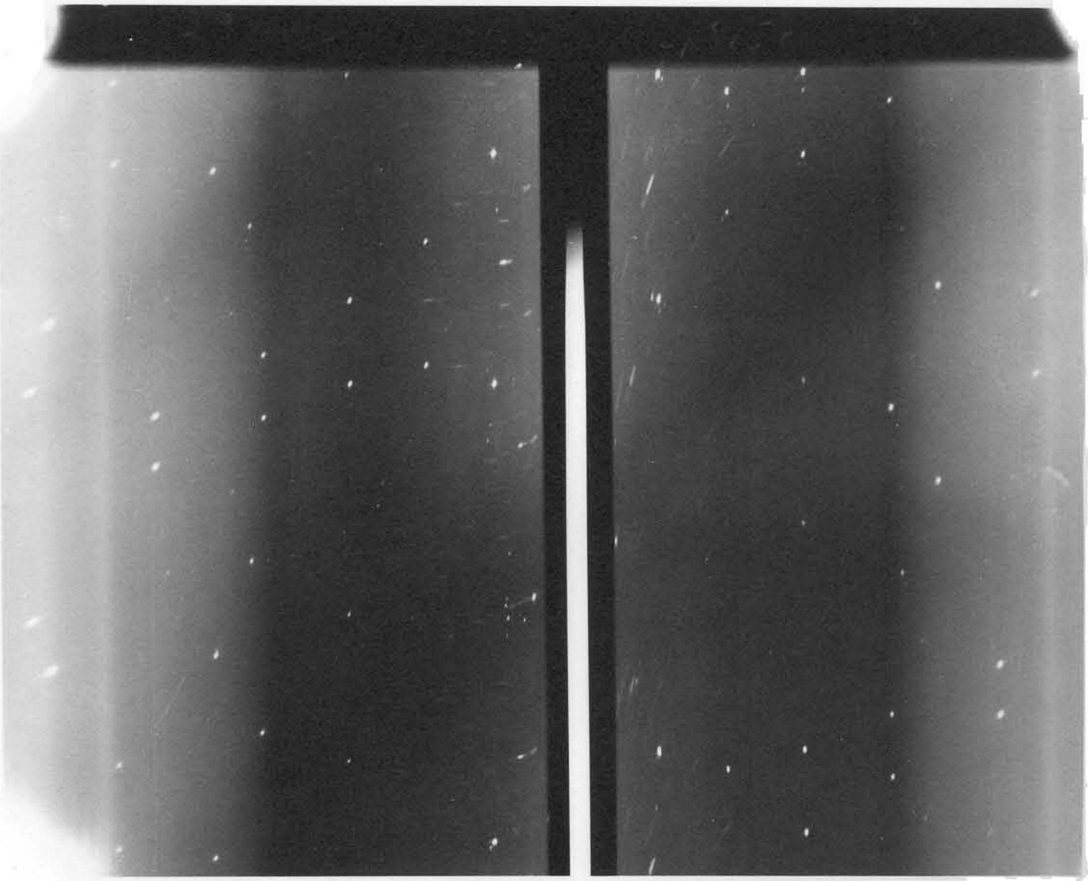

FIGURE 8.

WEISSENBERG PHOTOGRAPH OF THE (hk2)

RECIPROCAL LATTICE NET

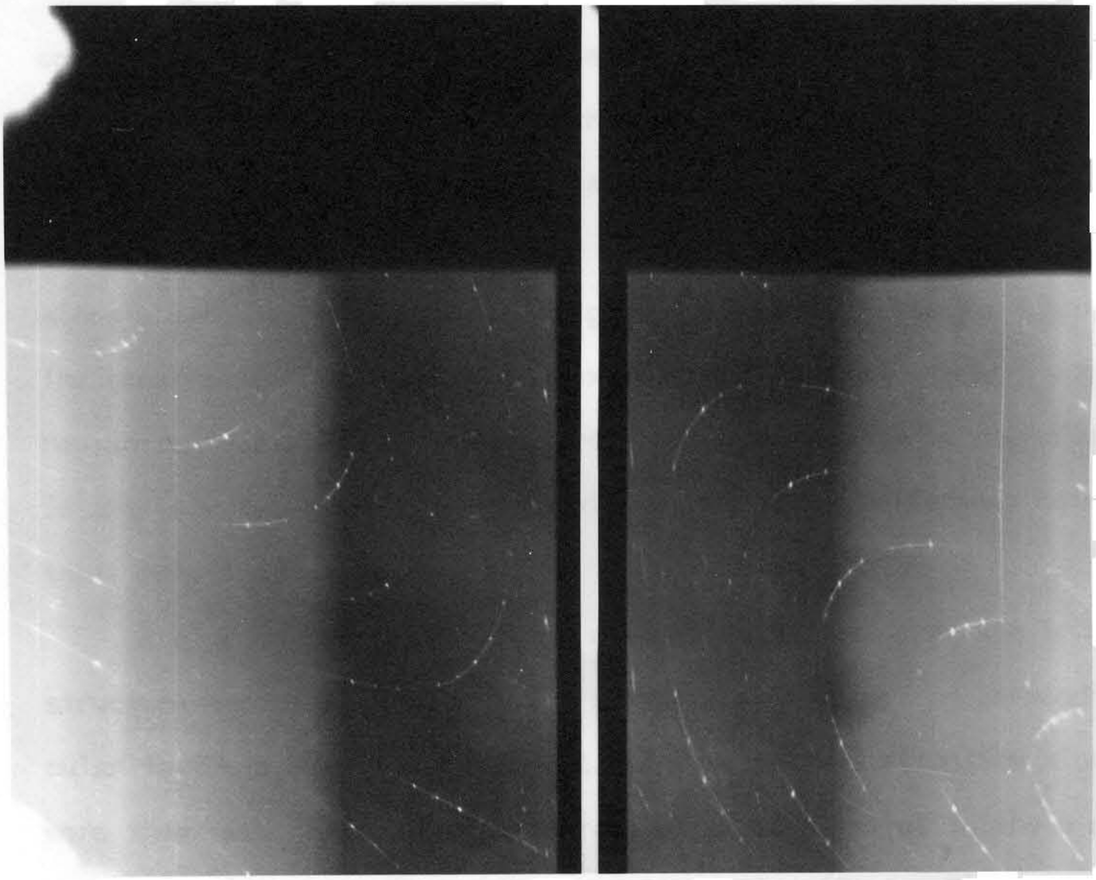

FIGURE 8 (continued).

WEISSENBERG PHOTOGRAPH OF THE (hk3)

RECIPROCAL LATTICE NET

this difference.

The occurrence of tails or streaks implied that the structure was to some extent disordered. In establishing the nature of this disorder it would, of course, be a matter of great importance that an explanation be given for the absence of the streaking on the reciprocal lattice nets with ℓ even.

In order for the disorder to cause streaks to occur which connect only diffraction maxima with the same k and ℓ indices it is necessary that it consists of a partial destruction of the perfect periodicity only in the direction of the a axis. Simultaneous destruction of the periodicity also in the directions of the b and c axes would not cause streaks but a general diffuse background all through reciprocal space. The occurrence of streaks, then, excludes the possibility of random replacement of silver atoms by strontium atoms or vice versa, which in any case would be unlikely in view of the great difference between their metallic radii.

A clue to the nature of the disorder was found when the trial structure was considered as built up from layers of atoms perpendicular to the c axis and $c_o/4$ apart. The silver and strontium atoms were then seen to form staggered rows of atoms parallel to the b axis and with silver and strontium atoms alternating (Figure 9). It was also seen that as far as the packing of the atoms is concerned, the silver and strontium atoms may be exchanged provided that there is a corresponding exchange of atoms in the layers $c_o/2$ away so that strontium atoms becoming nearest neighbors in the c direction is avoided (Figure 9). Similarly it is necessary that strontium and silver atoms

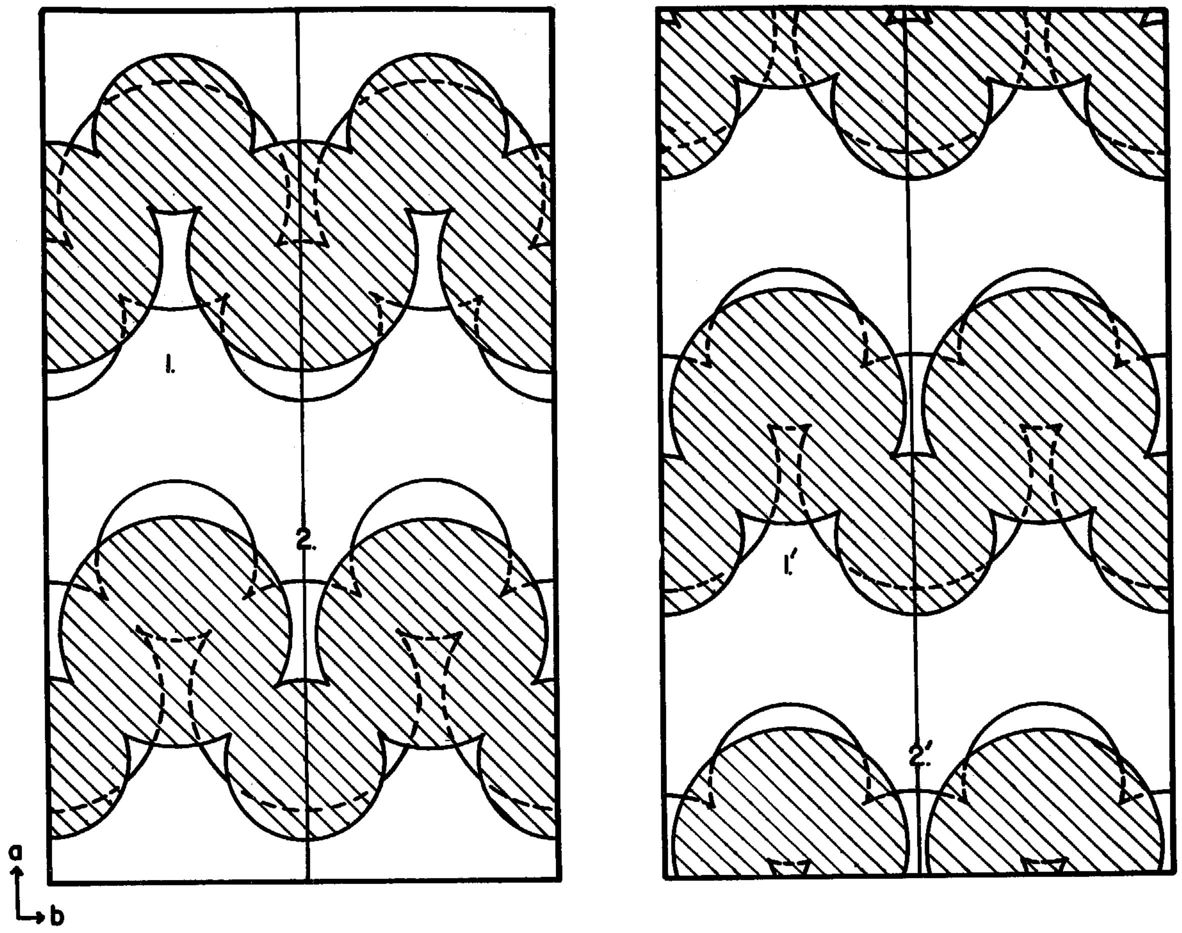

LAYERS AT $Z=0,\frac{1}{2}$

LAYERS AT $Z=\frac{1}{4},\frac{3}{4}$

FIGURE 9. THE PACKING OF THE TWO POSSIBLE TYPES OF ALTERNATE LAYERS AND THE EQUIVALENT PACKING SITES BETWEEN THESE TYPES OF ALTERNATE LAYERS

1,2 and 1',2' are sets of equivalent sites with respect to packing

▨ LAYERS AT $Z=0,\frac{1}{4}$ ○ LAYERS AT $Z=\frac{1}{2},\frac{3}{4}$

alternate in the staggered rows parallel to the b axis (Figure 9). An exchange of silver and strontium atoms with this kind of correlation between nearest neighbors in the b and c directions preserves the perfect periodicity in these directions so that streaks of the type observed must result. Furthermore, the correlation prevents the occurrence of streaks on the reciprocal lattice nets with ℓ even as the average value of the electron density at any two points (x,y,z) and (x,y,z+1/2) is insensitive to the exchange of atoms.

As the reciprocal lattice nets with ℓ odd show well defined maxima in addition to the streaks, the true structure must have an element of periodicity also in the a direction. The simplest explanation -- most likely also the correct one -- of the intensity distribution in reciprocal space is, then, that the true structure is identical with Structure II except that there are scattered through the structure imperfections involving the exchange of silver and strontium atoms as indicated. There will then be large volume elements of the structure (long in the a direction) and small elements (short in the a direction) within which the structure is exactly Structure II. The large elements give rise to the sharp maxima while the small elements which may be only a few cell edges long give rise to diffuse maxima connected by streaks. Each small element will, of course, give rise to diffuse maxima and subsidiary maxima as described by the Laue interference function, but the average effect of the subsidiary maxima will be observed as continuous streaks.

However, there is a second possibility. Inspection of the layers of atoms perpendicular to the c axis also shows that when the exchange of atoms is performed as described above but in a systematic fashion ordered structures arise differing from the trial structure but with equally good packing of the atoms (Figure 9). The two simplest of these ordered structures are discussed below. One of them has the space group C_{2v}^{7}-Pnm2, and the cell dimensions

$a_o' = 8.24$ Å ,
$b_o' = 4.792$ Å ,
$c_o' = 6.392$ Å .

The estimated positions of the atoms in the unit cell are

Sr_1 in 2(a): x,0,z;x,1/2,1/2+z; with $x_1 = 0.93$ and $z_1 = 0.00$;
Sr_2 in 2(a): with $x_2 = 0.43$ and $z_2 = 0.25$;
Ag_1 in 2(a): with $x_3 = 0.78$ and $z_3 = 0.50$;
Ag_2 in 2(a): with $x_4 = 0.28$ and $z_4 = 0.75$.

The relationship between the structure factors of this structure and those of structure II are

$$|F(hk\ell)| = 1/2\ |F(hk\ell)|^{II} \text{ for } \ell \text{ even,}$$
$$|F(hk\ell)| = 0 \text{ for } h, \ell \text{ odd ,}$$
$$|F(hk\ell)| = 1/\sqrt{2}\ |F(hk\ell)|^{II} \text{ for } h \text{ even and } \ell \text{ odd .}$$

The other structure has the space group C_{2v}^{16}-Ama2 and the cell dimensions

$a_o'' = 16.48$ Å ,
$b_o'' = 4.792$ Å ,
$c_o'' = 6.392$ Å .

The estimated positions of atoms in the unit cell are

Sr_1 in 4(b): (0,0,0;1/2,0,1/2) + x,1/4,z;$\bar{x}$,3/4,z; with $x_1 = 0.96$ and $z_1 = 0.00$;
Sr_2 in 4(b): with $x_2 = 0.21$ and $z_2 = 0.75$;

Ag_1 in 4(b): with $x_3 = 0.89$ and $z_3 = 0.50$;

Ag_2 in 4(b): with $x_4 = 0.14$ and $z_4 = 0.25$.

The relationship of the structure factors of this structure to those of structure II are

$$|F(hk\ell)| = |F(hk\ell)|^{II} \text{ for } \ell \text{ even },$$

$$|F(hk\ell)| = \sqrt{2}\,|F(hk\ell)|^{II} \text{ for } h, \ell \text{ odd },$$

$$|F(hk\ell)| = 0 \text{ for } h \text{ even and } \ell \text{ odd.}$$

It may now be assumed that the true structure consists of three kinds of volume elements with atomic arrangements corresponding to structure II and the two structures described above respectively. Similar to the previous case the small volume elements (having any of the three structures) incorporated in the composite structure cause the streaking.

This second type of disorder appears by no means unlikely, and it offers the advantage of providing an explanation to the observation that the observed structure factors of reflections with h even and ℓ odd appear stronger than the calculated structure factors while the opposite situation exists for reflections with h odd and ℓ odd. This would be the case if in the composite structure the C_{2v}^7 structure is relatively more important than the C_{2v}^{16} structure.

G. Refinement of the Structure

If the disorder involves only structure II the results of the least squares refinement described in section E are probably of significance even though the refinement ignored the evidence of disorder. If the disorder involves several structures a proper refinement would necessarily be much more complicated, and as it is doubtful that it would give a unique result with respect to the relative importance of the structures involved, such a refinement was never performed. In any case it is hardly possible that it would have yielded positional parameters substantially different from those already quoted.

H. Discussion of the Structure

Although the silver and strontium atoms are occupying nearly equivalent positions, the number of nearest neighbors that surround the silver atoms is only nine, seven of which are strontium atoms and two of which are silver atoms, while each strontium atom is surrounded by seventeen nearest neighbors, ten of which are strontium atoms and seven of which are silver atoms. The type of coordination is best visualized by inspection of Figure 6 which refers to structure II. The other two structures are left out of consideration, but it may be said that the coordination is very similar and the distribution of interatomic distances virtually the same. Table 12 lists the interatomic distances and the corresponding bond numbers. The sums of the bond numbers for the strontium atoms are 6.54 and 6.22 for Sr_1 and Sr_2 respectively in structure II while for the silver atoms the sums are 5.12 and 5.13 for Ag_1 and Ag_2 respectively. Although the values of the valence for silver agree satisfactorily with the expected valence of 5.44, the values for the strontium atoms are much larger than the expected value of 2. The high values of the calculated valence for strontium are possibly due to compression of the bonds and electron transfer.

It may be mentioned in conclusion that the structure of the inter-

Table 12

Interatomic Distances and Bond Numbers

Type of Distance	Length (Å)	Bond Number
Sr_1-Ag_1	3.40	0.569
	3.38	0.614
Sr_1-Ag_2	3.34	0.716
	3.33	0.745
Sr_2-Ag_1	3.34	0.716
	3.37	0.638
Sr_2-Ag_2	3.42	0.526
	3.40	0.569
Sr_1-Sr_1	4.18	0.259
	4.79	0.025
Sr_2-Sr_2	4.17	0.270
	4.79	0.025
Sr_1-Sr_2	4.40	0.111
	4.43	0.100
	4.10	0.352
Ag_1-Ag_2	2.93	0.380

metallic compound NiTh has recently been determined (8). The structure of this compound has the same space group and the same number of atoms per unit cell as structure II, but the atomic positions are quite different which is perhaps somewhat surprising in view of the fact that the radius ratio of thorium and nickel (1.45) is very nearly the same as that of strontium and silver (1.49).

V. THE INTERMETALLIC COMPOUND Ag_2Sr_3

A. Materials

An alloy of the composition Ag_2Sr_3 was prepared from 9.01 gm. of silver and 11.00 gm. of strontium by the same method and from the same materials used to prepare the Ag_5Sr alloy. The composition of a representative sample of the alloy found by chemical analysis agreed within 1% with the composition Ag_2Sr_3.

The alloy was brittle and grayish in appearance. It was very reactive and on exposure to air rapidly disintegrated into a black powder.

B. X-ray Photography and Laue Symmetry

It was very difficult to isolate single crystal fragments of this alloy suitable for X-ray photography. About eighty fragments of the alloy were mounted in glass capillaries as was done with the fragments of the AgSr alloy.

Laue photographs of the fragments showed that all but one of them were polycrystalline. The single crystal fragment displayed Laue symmetry D_{2h}-mmm. With a Supper Weissenberg goniometer two rotation photographs with rotation about one of the orthorhombic axes (labeled the a axis) and Weissenberg photographs with $h = 0,1,\ldots,10,15,20,25,30$ and 35 were taken of this crystal using copper K_α radiation. The diffraction pattern of a sodium chloride powder sample was also photographed on one of the rotation photographs for calibration. Precession photographs of the reciprocal lattice nets with $k = 0$ and 1 and $\ell = 0,1$ and 2 were also obtained with this crystal using molybdenum K_α radiation. A Supper precession goniometer was used. A Straumanis type rotation photograph of the net with h = 0 was taken using copper K_α radiation. The diffraction pattern of a quartz powder sample was photographed on the same film for calibration purposes. Powder photographs of a crushed alloy sample were obtained with a Philips powder camera (Straumanis type) using copper K_α radiation.

C. The Unit Cell Dimensions

The approximate unit cell dimensions were obtained from the rotation and Weissenberg photographs. They were

$$a_o = 42.0 \text{ Å} ,$$
$$b_o = 4.80 \text{ Å} ,$$
$$c_o = 6.40 \text{ Å} .$$

As in the case of the AgSr compound the powder data could not be used as the basis of a refinement of the lattice constants because of the heavy background on the powder photographs. The refinement consequently had to be based on single crystal data. Furthermore, because of the similarity of the powder pattern of the Ag_2Sr_3 phase with that of the AgSr phase, it was not possible to draw a definite conclusion regarding the composition of the single crystal even though all the measurable diffraction arcs except two moderately weak arcs appeared to match the single crystal data both with respect to Bragg angle and intensity.

Accurate values of the parameters b_o and c_o were obtained from precise measurements of the Straumanis type rotation photograph of the reciprocal lattice net with h = 0. This refinement was carried out in exactly the same way as the refinement of the b_o and c_o parameters of the AgSr structure. The results of the refinement based on data gathered at 25° C. were

$$b_o = 4.792 \pm 0.001 \text{ Å} ,$$

$$c_o = 6.391 \pm 0.001 \text{ Å} .$$

The uncertainties are the probable errors.

Table 13 lists the calculated and observed Q's with their differences and corresponding weights. The differences again indicated that there was a systematic error present in the observed data (probably due to absorption). However, this error was found to be small enough to be neglected.

A more accurate value of a_o was obtained in exactly the same manner as the corresponding parameter of the AgSr structure. The value of a_o determined from data obtained at 25° C. was

$$a_o = 41.59 \pm 0.05 \text{ Å}$$

where the uncertainty is the probable error.

Figure 10 shows the values of a_o obtained from the individual measurements plotted against sin θ. There is no indication of systematic errors in the data and the refined value of a_o should require no correction.

D. The Atomic Arrangement and the Unit Cell Contents

Very early in the investigation it became clear that the Ag_2Sr_3 and AgSr structures were closely related. Both structures have orthorhombic symmetry and the cell dimensions are related in a very simple way. The b_o and c_o parameters are practically the same, and the a_o parameter of the Ag_2Sr_3 structure is almost exactly 5/2 times larger

Table 13

The Calculated and Observed Values of Q

Index	Weight	Q_{obs}	Q_{calc}	$Q_{obs} - Q_{calc}$
020_{β}	3.28	0.1748	0.1742	0.0006
020_{α}	2.75	0.1750	0.1742	0.0008
004_{β}	1.64	0.3925	0.3918	0.0007
004_{α}	1.42	0.3922	0.3918	0.0004
024_{β}	1.26	0.5670	0.5660	0.0010
024_{α}	1.13	0.5670	0.5660	0.0010
040_{β}	1.13	0.6962	0.6967	-0.0005
040_{α}	1.03	0.6970	0.6967	0.0003
044_{β}	1.00	1.0882	1.0885	-0.0003
044_{α_1}	1.09	1.0884	1.0885	-0.0001
044_{α_2}	1.10	1.0886	1.0885	0.0001
008_{β}	1.37	1.5671	1.5670	0.0001
060_{β}	1.37	1.5671	1.5677	-0.0006
028_{β}	1.91	1.7407	1.7412	-0.0005

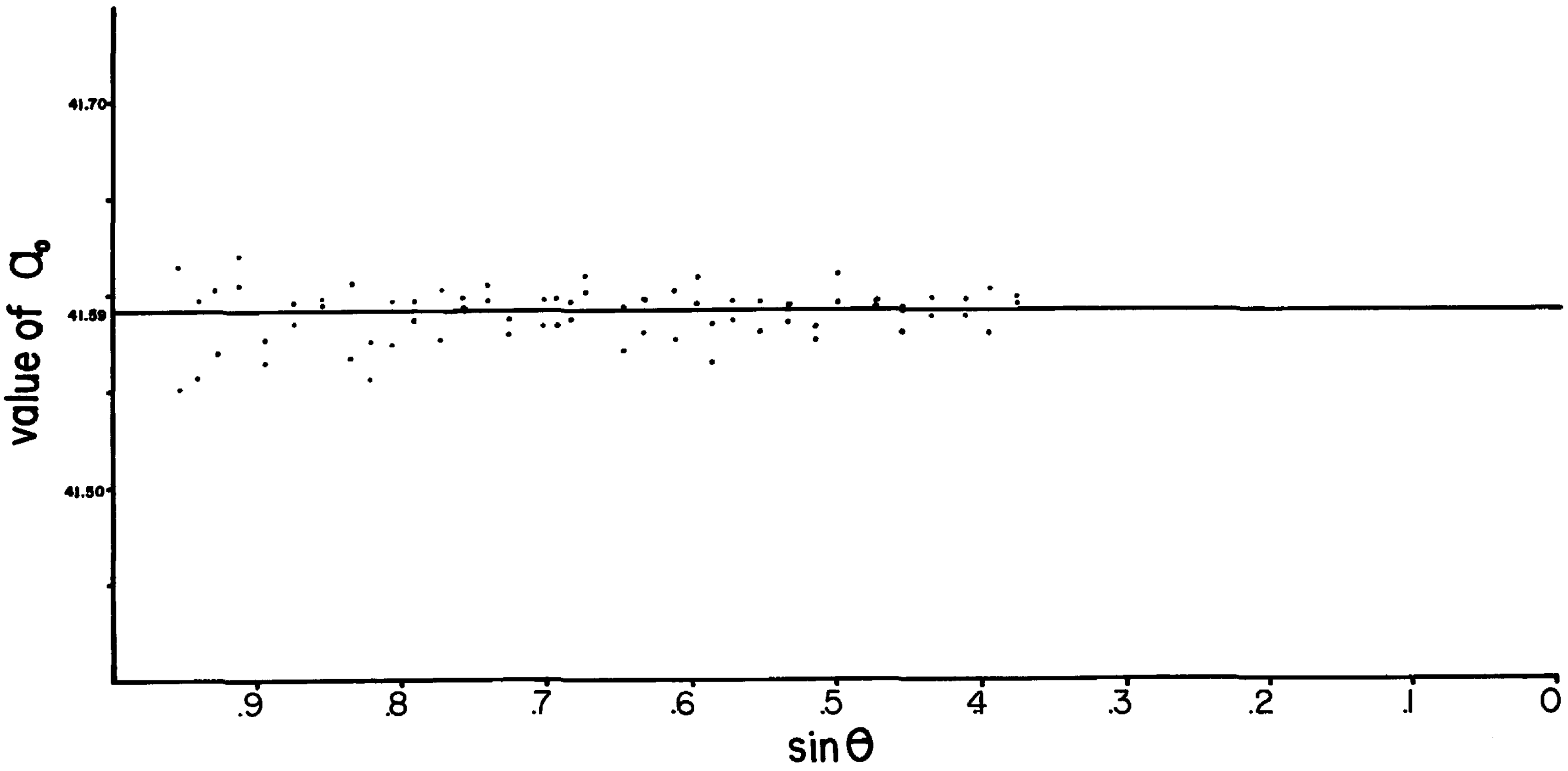

FIGURE 10. A PLOT OF a_0 AS A FUNCTION OF SIN θ

than that of the AgSr structure. There is also a striking similarity in the distribution of diffraction intensities. This similarity is particularly striking for the reciprocal lattice nets with ℓ even which are virtually indistinguishable from each other. It was therefore a reasonably safe conclusion that the atomic arrangements are the same in the two structures if no distinction is made between silver and strontium atoms and that there are consequently 40 atoms per unit cell in the Ag_2Sr_3 structure. The difference between the two structures, then, must consist of a difference in the distribution of silver and strontium atoms over the atomic sites which are all the same in the two structures (ignoring small differences in the atomic coordinates). If the composition is given by the formula Ag_2Sr_3, there would then be 16 silver atoms and 24 strontium atoms per unit cell. This conclusion is not confirmed too well by density measurements. The calculated density is 4.99 gm. cm.$^{-3}$ while the experimental density of the alloy as found by pycnometric methods was only 4.50 gm. cm.$^{-3}$. It is possible that the great reactivity of the alloy led to a very poor experimental density.

There seems to be no method for finding the distribution of strontium and silver atoms over the atomic sites except the trial and error method. The observation that the reciprocal lattice nets with ℓ odd are also similar to those of the AgSr structure is undoubtedly of great value in reducing the number of possible trial structures but so far only a little progress has been made. If the atomic sites are occupied as required by the formula Ag_2Sr_3, the accommodation of more strontium atoms than silver atoms would make it necessary that some of the rows of atoms parallel to the c axis be considerably staggered — more staggered than appears plausible after inspection of the (hk0) diffraction intensities. This latter point is particularly puzzling. There is no evidence of disorder in the structure.

VI. REFERENCES

(1) F. Weibke, *Z. Anorg. Allg. Chem.*, (1930), *193*, 297-310.

(2) *Metals Handbook*, (American Society for Metals, 1948), 1148, 1218.

(3) H. Nowotny, *Z. Metallkunde*, (1942), *34*, 247-253.

(4) A. Miller, Ph. D. Thesis, California Institute of Technology, (1957), 227.

(5) W. Haucke, *Z. Anorg. Allg. Chem.*, (1940), *244*, 17-22.

(6) W. Fülling, K. Moeller and R. Vogel, *Z. Metallkunde*, (1942), *34*, 253-254.

(7) F. Endter and W. Klemm, *Z. Anorg. Chem.*, (1943), *252*, 64-66.

(8) J. Florio, N. Baenziger and R. Rundle, *Acta Cryst.*, (1956), *9*, 367-372.

(9) L. Pauling, *J. Am. Chem. Soc.*, (1947), *69*, 542-553.

(10) L. Pauling, *The Nature of the Chemical Bond*, Cornell University Press, New York (1948), 409.

(11) C. Gottfried and F. Schossberger, *Strukturbericht*, (1933-35), *3*, 28.

(12) P. Schlicta, Ph. D. Thesis, California Institute of Technology, (1956), 106-119.

(13) M. E. Jones, Ph. D. Thesis, California Institute of Technology, (1953), 32-43.

(14) R. Kiessling, *J. Electrochem. Soc.*, (1951), *98*, 166-170.

(15) W. Hofman and W. Jäniche, *Z. Phys. Chem.*, (1936), *B-31*, 214-222.

(16) F. Bertant and P. Blum, *Acta Cryst.*, (1951), *4*, 72.

(17) C. J. Smithells, *Metals Reference Book*, (1949), 181-194.

(18) M. Straumanis and A. Ieviņš, *Z. Phys.*, (1936), *102*, 353-359.

(19) J. J. Lange, M. J. Robertson and I. Woodward, *Proc. Roy. Soc. (London)*, (1939), *A171*, 398-410.

(20) A. J. Bradley, *Proc. Phys. Soc. (London)*, (1935), *47*, 879-899.

VII. PROPOSITIONS

1. The controversy over the mechanism underlying the operation of the glass electrode can be resolved by the use of a radioactive tracer such as tritium.

2. A satisfactory understanding of the nature of the solutions of alkali metals and alkaline earth metals in liquid ammonia has not been obtained yet. From a solution of calcium in liquid ammonia the solid compound $Ca(NH_3)_6$ can be precipitated. This presumably crystalline compound has the same optical and electrical properties as the liquid solution of calcium in ammonia (1 and 2). It is proposed that an attempt be made to determine the crystal structure of the solid compound in the hope that the results will be of value in elucidating the properties of these metal ammonia solutions.

3. Ethylenediammine tetraacetic acid is very insoluble in acid aqueous solutions. Thus in acid solutions it is a very poor chelating agent. Aliphatic sulfonic acids are completely soluble even if the aliphatic chain is large so that substitution of an aliphatic sulfonic acid for some of the acetic acid should result in a vastly improved chelating agent particularly in acid solutions.

4. In preparing intermetallic compounds it is common practice to let the eutectic mixture solidify with the crystals of the intermetallic compound. In general it would be more satisfactory if the intermetallic compound could be obtained alone. A technique is suggested that should make this possible in many cases.

5. L. Alders in his book poses two questions dealing with the extraction of a solute from a solution by a limited quantity of an im-

miscible solvent in a cross-current extraction process (3). They are

(a) What portion of the total amount of the immiscible solvent available must be used in each stage to obtain the greatest efficiency of extraction?

(b) Must extraction be effected in many or in few stages to obtain the greatest efficiency of extraction?

His mathematical solutions of these questions do not seem adequate. Two alternate solutions are offered.

6. In a recent structure investigation of the α phase in the vanadium-aluminum system it was found that the structure of the α phase contains holes large enough to accomodate atoms (4). This is contrary to the generally valid rule of efficient packing in metals and alloys and does not seem reasonable. It is recommended that the structure of the α phase be re-investigated.

7. It is conjectured by botanists that desert lichens are able to absorb enough moisture from evening dews or perhaps directly from the air at night when the relative humidity is reasonably great to maintain their vitality. This hypothesis could be easily tested in a laboratory under controlled conditions.

8. A modification of the layer line screens of the Supper Weissenberg goniometers is proposed. With this modification the width of the slit can be reduced without limiting the range of possible equi-inclination angles. Reduction of the width of the slit would cut down the amount of general background on the photographs and also extend the usefulness of the goniometer to crystals with large cell dimensions.

9. It is a known fact that X-rays (characteristic radiation) can

be excited with positive ions impinging on the surface of a material (5,6 and 7). No or negligible bremsstrahlung is produced. Such a source will produce essentially pure, unpolarized characteristic radiation. Therefore an X-ray source of this type would be superior for X-ray diffraction work to those ordinarily used. Since very little is known about production of X-rays by positive ions, it is proposed that an investigation be made to determine if such a source of X-rays is practical for X-ray diffraction work.

10. In the qualitative analysis scheme of Noyes if both silver and mercurous ions are present, freshmen invariably get no test for silver. This is due to the fact that mercury metal reduces the silver present in any form to silver metal thus removing it from solution and subsequently leading to negative or inconclusive tests for silver. To avoid this difficulty the following modification can be made

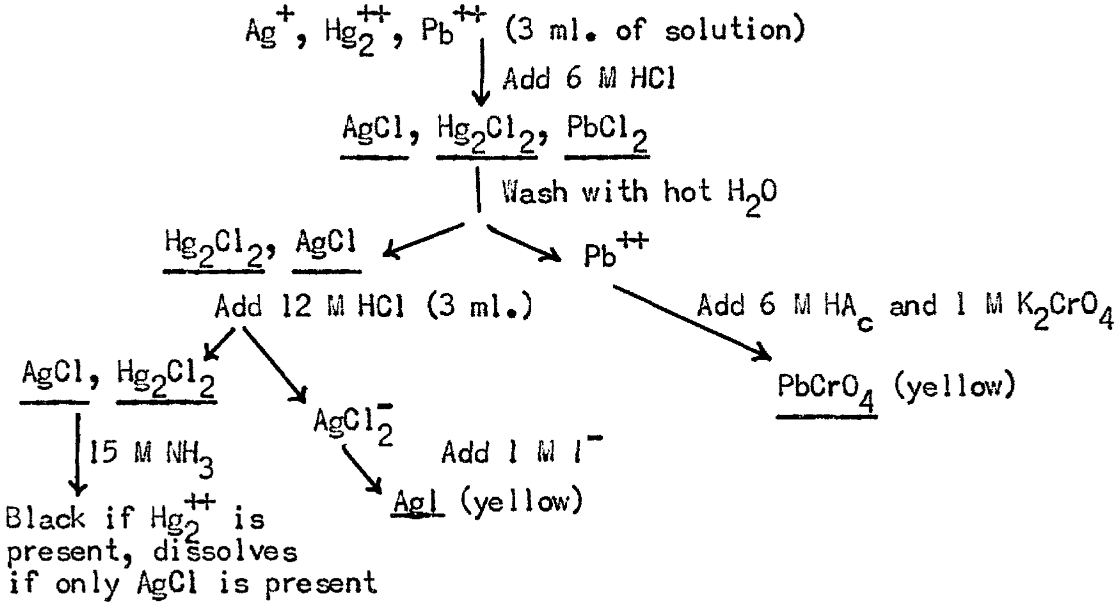

Note: Small amounts of Pb^{++} can be carried through without interfering with the tests for either Ag^+ or Hg_2^{++}.

References to Propositions

(1) L. Audrieth and J. Kleinberg, *Non-Aqueous Solvents*, (1953), Chapter 6.

(2) C. A. Kraus, *J. Am. Chem. Soc.*, (1907), *29*, 1557-1571; (1908), *30*, 653-668; (1908), *30*, 1323-1344; (1914), *36*, 864-877; (1921), *43*, 749-770; and (1921), *43*, 2529-2539.

(3) L. Alders, *Liquid-Liquid Extraction*, (1955), 80.

(4) P. J. Brown, *Acta Cryst.*, (1957), *10*, 133-135.

(5) W. Bothe and H. Fränz, *Z. Phys.*, (1928), *52*, 466-484.

(6) C. Gerthsen and W. Reusse, *Phys. Zeits.*, (1933), *34*, 478-482.

(7) M. S. Livingston, F. Genevese and E. J. Konopinski, *Phys. Rev.*, (1937), *51*, 835-839.